



Assessment of vanadium distribution in shallow groundwaters

Olivier Pourret, Aline Dia, Gérard Gruau, Mélanie Davranche, Martine Bouhnik-Le Coz

► To cite this version:

Olivier Pourret, Aline Dia, Gérard Gruau, Mélanie Davranche, Martine Bouhnik-Le Coz. Assessment of vanadium distribution in shallow groundwaters. Chemical Geology, 2012, 294-295, pp.89-102. 10.1016/j.chemgeo.2011.11.033 . insu-00671076

HAL Id: insu-00671076

<https://hal-insu.archives-ouvertes.fr/insu-00671076>

Submitted on 16 Oct 2012

HAL is a multi-disciplinary open access archive for the deposit and dissemination of scientific research documents, whether they are published or not. The documents may come from teaching and research institutions in France or abroad, or from public or private research centers.

L'archive ouverte pluridisciplinaire **HAL**, est destinée au dépôt et à la diffusion de documents scientifiques de niveau recherche, publiés ou non, émanant des établissements d'enseignement et de recherche français ou étrangers, des laboratoires publics ou privés.

ASSESSMENT OF VANADIUM DISTRIBUTION IN SHALLOW GROUNDWATERS

Olivier Pourret^{1*}, Aline Dia^{2#}, Gérard Gruau²,
Mélanie Davranche² and Martine Bouhnik-Le Coz²

¹ HydrISE, Institut Polytechnique LaSalle Beauvais

19 rue Pierre Waguet

60026 Beauvais Cedex, France

² Géosciences Rennes, Université Rennes 1, CNRS

Campus de Beaulieu

35042 Rennes Cedex, France

Keywords: vanadium, natural waters, ultrafiltration, speciation calculation, groundwater-rock interaction, redox change

*Tel: +33 344 068 979; Fax: + 33 344 068 970; E-mail address: olivier.pourret@lasalle-beauvais.fr.

#Tel: +33 223 235 650; Fax: + 33 223 235 787; E-mail address: aline.dia@univ-rennes1.fr.

Abstract

Shallow groundwater samples (filtered at 0.2 μm) collected from a catchment in Western France (Petit Hermitage catchment) were analyzed for their major- and trace-element concentrations (Fe, Mn, V, Th and U) as well as their dissolved organic carbon (DOC) concentrations, with the aim to investigate the controlling factors of vanadium (V) distribution. Two spatially distinct water types were previously recognized in this catchment based on variations of the rare earth element (REE) concentrations. These include: (i) DOC-poor groundwater flowing below the hillslope domains; this type has low V contents; and (ii) DOC-rich groundwater originating from wetlands, close to the river network; the latter water type displays much higher V concentrations. The temporal variation of the V concentration was also assessed in the wetland waters; the results show a marked increase in the V content at the winter-spring transition, along with variations in the redox potential, and DOC, Fe and Mn contents.

In order to allow the study of organo-colloidal control on V partitioning in water samples, ultrafiltration experiments were performed at different pore size cut-offs (30 kDa, 10 kDa and 5 kDa). Two shallow, circumneutral waters were sampled: one was both DOC- and Fe-rich and the other was DOC-rich and Fe-poor. In terms of major- and trace-cations and DOC concentrations, the data were processed using an ascendant hierarchical classification method. This revealed the presence of two main groups: (i) a "truly" dissolved group (Na, K, Rb, Ca, Mg, Ba, Sr, Si, Mn, Co, Ni, Cr, Zn and Ni), and (ii) a colloidal group carrying DOC, Fe, Al, Pb, Cu, REE, U, Th and V. Vanadium has an unpredictable behaviour; it can be either in the organic pool or in the inorganic pool, depending on the sample.

Moreover, V speciation calculations - using Model VI and SCAMP - were performed on both samples. Speciation modelling showed approximately the same partitioning feature of these elements as compared to ultrafiltration data, namely: a slight change of the V speciation in groundwaters along the studied topographic sequence.

This implies that vanadium in hillslope groundwater wells occurs as a mixing of organic and

inorganic complexes, whereas V in wetland groundwater wells comprises mainly organic species. Using the dataset described above, factors such as aquifer-rock composition or anthropogenic input were demonstrated to probably play a minor role in determining the V distribution in shallow groundwaters. Although an anthropogenic impact can be ruled out at this local scale, we cannot preclude a perturbation in the global V cycle. Most likely, the two dominant factors involved are the organic matter content and the redox state either promoting competition with Fe-, Mn-oxides as V carriers in groundwater or not. In this context, it appears challenging to determine whether organic matter or redox-sensitive phases are the major V carriers involved, and a further study should be dedicated to clarify this partition, notably to address the processes affecting large-scale V transport.

1. Introduction

Vanadium (V) is a naturally occurring element in air, soil, plants and water. Its average content in the earth's crust is approximately 0.0136% (Greenwood and Earnshaw, 1997). Vanadium in trace amounts represents an essential element for normal cell growth, but it may cause adverse effects when its concentration is much greater than a few tenths of μg per litre (Hope, 1997). Most data on the release of V into the environment have been related to industrial activities, especially from oil refineries and power plants using V-rich fuel oil and coal (e.g., Moskalyk and Alfanti, 2003 and references therein). Crude oil is enriched in V with respect to many other trace elements, with concentrations occasionally exceeding 1 mg L^{-1} (Hope, 1997). Thus, the fraction of dissolved V in surface waters might be an environmental indicator of oil combustion or pollution. Such pollution sources may be responsible for appreciable amounts of V into the environment, well above the natural background levels associated with rock weathering and sediment leaching (Hope, 1997; Lowenthal et al., 1992; Rühling and Tyler, 2001). Fluvial dissolved V concentrations might also be indicative of the types of rocks being weathered or, of

the nature of the weathering process. Shiller and Boyle (1987) presented an overview of the behaviour of dissolved V in rivers and estuaries. Shiller and Boyle (1987) and Shiller and Mao (2000) concluded that weathering rate and type of source rock, rather than solution chemistry or anthropogenic influences, appeared to be the important controlling factors on fluvial dissolved V concentrations.

Vanadium has several oxidation forms between -1 and +5. Vanadium(II) is particularly unstable in the environment (Wehrli and Stumm, 1989). Vanadium(III) is more stable than V(II), but it is also gradually oxidized by the air or dissolved oxygen. Vanadium(V) is expected to be the prevailing form in waters exposed to atmospheric oxygen, whereas V(IV) may be present in reducing environments. The oxidation rate of V(IV) to V(V) and the equilibrium between these two species in aqueous solution depend on several factors, such as pH, V concentration, redox potential, the ionic strength of the aqueous system and biological activity (e.g., Wang and Sanudo Wilhelmy, 2009). In water, V(IV) is commonly present as a vanadyl cation [VO^{2+} , $\text{VO}(\text{OH})^+$], whereas V(V) exists as a vanadate oxyanion (H_2VO_4^- , HVO_4^{2-}) (Wanty and Goldhaber, 1992). VO^{2+} is strongly adsorbed on solid phases, including organic and oxyhydroxide phases (Wehrli and Stumm, 1989). Adsorption of anionic V (H_2VO_4^- , HVO_4^{2-}) is much lower than the cations; however, VO^{2+} solubility may be greatly increased through complexation with organic matter (Lu et al., 1998; Szalay and Szilagyi, 1967). While V(IV) is not thermodynamically stable at $\text{pH} > 7$, complexation by various organic and inorganic species may considerably increase its stability (Wanty and Goldhaber, 1992). Eventually, the V(V) oxidation state ion is more toxic than the V(IV) ion (Hope, 1997; Hope, 2008).

A recent study on the geochemistry of V has emphasized the redox features of this element (Wright and Belitz, 2010), which makes it more soluble in oxidizing waters than in reducing waters (Wehrli and Stumm, 1989). As a consequence, fluvial dissolved V concentrations might be an indicator of inputs from reducing sources within river drainage systems (Shiller, 1997; Sugiyama, 1989). Additionally, this difference in solubility appears to be

104 an important contributing factor to the enrichment of V in organic-rich reducing sediments (Breit
105 and Wanty, 1991). Other studies have investigated V geochemistry as a potential
106 paleoceanographic tool. For example, Francois (1988) and Calvert and Pedersen (1993)
107 examined the V accumulation in sediments as an indicator of past reducing conditions in specific
108 oceanic regions. Hastings et al. (1996) have also evaluated the incorporation of V into biogenic
109 carbonate phases as a possible indicator of the past oceanic conditions. Seeking a better
110 understanding of the processes that result in V removal into organic-rich sediments, Emerson and
111 Husted (1991) assessed V distributions in oxygen-depleted present-day natural waters. They
112 found that dissolved V concentrations were generally lower in anoxic basins than in oxic
113 seawater, due to V removal into anoxic sediments. In addition to the study by Emerson and
114 Husted (1991), other authors (e.g., Szalay and Szilagyi, 1967) have suggested that organic
115 matter may play a role in modifying vanadium's redox behaviour through the reduction of V(V)
116 by humic acid and by the competition of organics with solid surfaces for V(IV). However, in
117 order to explain oceanic changes in terms of dissolved V, the processes majorly affecting the
118 oceanic sources of this element must also be understood (i.e., rivers, groundwaters).

119 This study reports temporal and spatial variations of V shallow groundwaters from wells located
120 along a transect set perpendicular to the topographic slope (hereafter denoted as toposequence)
121 set up in a small catchment in France. Ultrafiltration and speciation modelling of representative
122 samples of this toposequence, using the Windermere Humic Aqueous Model (WHAM) including
123 both Humic Ion-binding Model VI (Tipping, 1998) and the Surface Chemistry Assemblage
124 Model for Particles (SCAMP; Lofts and Tipping, 1998), are also presented. Such modelling
125 permits the calculation of equilibrium chemical speciation for waters in which natural organic
126 matter plays a significant role. The catchment studied here was chosen as a suitable site for V
127 investigation because information in terms of hydrogeology, hydrochemical and trace elements
128 such as rare earth elements (REE) settings is already available (Clément et al., 2003; Gruau et al.,
129 2004). In this context, the main aims of this work are to address the respective influence of

source-rock composition, redox changes and organic matter on the distribution of V in shallow groundwaters.

2. Material and methods

2.1 Site description

The study was conducted between winter 1998 and spring 2004 in a riparian ecosystem (the “*Le Home*” toposequence) located along a small tributary (Petit Hermitage Creek) in western France (48.3°N, 1.3°W), at an altitude of ca. 20 m above sea level (Fig. 1). The study site was located within a 14 km² drainage basin. The region has an oceanic climate characterized by mild, humid weather throughout the year. Annual rainfall ranged between 850 and 900 mm during the study period. The mean discharge of the stream is approximately 90 L s⁻¹. The stream hydrological regime is characterized by low permanent flow during dry periods (i.e., late spring and summer), and rapid and significant flood events during high water periods (i.e., late winter and early spring). The upland-riparian boundary is characterized by a steep 2–3 m drop in elevation from the surrounding fields into the riparian ecosystem (Fig. 1). The catchment drained by the riparian wetland is mainly agricultural with crops and grass fields for cattle. At the time of the study, the eastern part of the upslope was under perennial grassland mown for hay and grazed by suckling cows and calves for only a few weeks per year. The western part of the upslope was a crop field (maize/wheat) with intensive agricultural practices. Fertilizer application rates were high, [N]³ 200 kg ha⁻¹ year⁻¹, which resulted in high groundwater NO₃⁻-N concentrations ranging from 10 to 20 mg L⁻¹ (Clément et al., 2003; Gruau et al., 2004). The geological substratum of the catchment is granite in the upstream part (Villegardier Forest) and micaschist (Proterozoic schist) in the downstream part where the study site is located. Compared to the deeper fresh rocks, the upper 10–20 m have been weathered into a higher clay content. The wetland is filled with late Phanerozoic clay-rich alluvium.

2.2 Sampling and field measurements

Wetland groundwater samples (F14 well) were recovered weekly from January 1999 to June 1999 for the temporal and spatial variation study. Groundwater samples flowing below the upland/wetland transition zone (F5 and F7 wells) were collected twice, in February 1998 and January 1999, while the upland P11 well was sampled only once, in January 1999 (Fig. 1). Wetland groundwaters (F14 well) and other samples flowing below the upland/wetland transition zone (F7 well) were sampled in November 2004 for the ultrafiltration experiments. These water samples were immediately filtered on site using 0.2 μm cellulose acetate filters. Filters were pre-cleaned with ultrapure water to prevent any contamination (Bouhnik-Le Coz et al., 2001; Petitjean et al., 2004). Temperature, pH and Eh were measured on site. The pH was measured with a combined Sentix 50 electrode; the accuracy of the pH measurement is ± 0.05 . Eh was measured using a platinum combination electrode (Mettler Pt 4805). Electrodes are inserted into a cell constructed to minimize diffusion of atmospheric oxygen into the sample during measurement. Eh values are presented in millivolts (mV) relative to the standard hydrogen electrode. The accuracy of Eh measurement is ± 5 mV.

2.3 Ultrafiltration set-up description and chemical analyses

Ultrafiltration experiments were performed on two samples recovered from the F7 and F14 wells using 15 mL centrifugal tubes (Millipore Amicon Ultra-15) equipped with permeable membranes of decreasing pore sizes of 30 kDa, 10 kDa, and 5 kDa (1 Da = 1 g mol⁻¹ for H) for the separation of the colloidal bound elements. Metal-colloid complexes are retained by the ultrafiltration membrane, whereas free ions and smaller chemical complexes pass into the ultrafiltrate. The degree of metal-colloid complexation is usually determined from the metal concentration in the ultrafiltrate relative to the original solution. Each centrifugal filter device

was washed and rinsed with HCl 0.1 mol L⁻¹ and ultra-pure (MilliQ) water two times before use. The starting filtrates were passed through a 0.2 µm filter, and then aliquots of these filtrates were passed through membranes of smaller sizes. All ultrafiltrations of the 0.2 µm filtrates were done in parallel. The centrifugations were performed using a Jouan G4.12 centrifuge equipped with a swinging bucket rotor at about 3,000 g for 20 minutes for the 30 kDa and 10 kDa filters and 30 minutes for the 5 kDa filters, respectively. All experiments were carried out at room temperature (~20 ± 2°C).

Major cations and trace elements concentrations were determined by ICP-MS (Agilent Technologies HP4500) at the University of Rennes 1. Quantitative analyses were carried out by external calibration (three points) by using mono- and multi-element standard solutions (Accu Trace Reference, USA) with major- and trace-element concentrations similar to that of the analyzed samples. Indium was used as an internal standard at a concentration of 100 µg L⁻¹ in order to correct for instrumental drift and matrix effects. The measurement bias for the determination of the concentration of major- and trace-elements was assessed in a previous work by the analysis of the SLRS-4 certified reference material (river water); a bias < 2% was obtained for all analytes (Pédrot et al., 2008; Pourret et al., 2007b; Yeghicheyan et al., 2001). Dissolved organic carbon concentrations were determined using a Shimadzu 5000 TOC analyzer (Université de Rennes 1). A measurement bias of ± 5% was obtained by the analysis of a freshly prepared standard solution of potassium biphtalate. Total alkalinity was determined by potentiometric titration with an automatic titrating device (794 Basic Titrino Methrom). Major anion (Cl⁻, SO₄²⁻ and NO₃⁻) concentrations were measured by ionic chromatography (Dionex DX-120) with a bias below 4%. Carbonate alkalinity was determined by potentiometric titration with an automatic titrator (Basic Titrino Metrohm).

It is worth noting that the ultrafiltration procedure prevents the calculation of the mass balance using the ratio between the filtrate and the retentate because the retentate volumes are limited (0.2 mL). However, as the same material was used for all filtrations, molecular size

exclusion rather than adsorption onto membranes should control the colloid distributions between ultrafiltrates.

In our study, all ultrafiltrations were performed in duplicate. A good repeatability was observed for DOC and both major and trace element concentrations. The relative difference between duplicates was generally < 5% for most elements except for some trace elements in the lower pore size cut-off fraction (i.e., in the < 5 kDa fraction, about 10%). Further information on the ultrafiltration procedure can be found in Pourret et al. (2007b). The possible adsorption of major and trace inorganic species onto the membrane or cell walls was also monitored. For this purpose, inorganic multi-element standard solutions - whose concentrations were representative of that of the studied groundwaters - were ultrafiltered several times (Pourret et al., 2007b). The results showed that between 92.99% (for Pb) and 99.99% (for Mg) of the major- and trace-elements present in solutions were recovered in the ultrafiltrates (96.13% for V), demonstrating that neither the major nor trace elements were adsorbed onto the membranes or walls of the cell devices.

In order to lessen the cross-contamination of any of the analytical steps (sampling, filtration, storing and analysis), the samples were stored in acid-washed Nalgene polypropylene containers before analyses. The blank levels were lower than 2% of the measured concentrations for all studied elements, except for DOC (< 6%).

2.4 WHAM 6, Model VI and SCAMP description

WHAM 6 (version 6.0.10) was used to calculate V speciation. Predictions for the equilibrium metal binding by environmental colloids made for the present study were done using the combined WHAM-SCAMP speciation code. WHAM-SCAMP is able to provide a full description of solid-solution speciation by incorporating two main codes: (1) the Windermere Humic Aqueous Model (WHAM) to calculate the equilibrium solution speciation (Tipping,

1994), and (2) the Surface Chemistry Assemblage Model for Particles (SCAMP) to calculate the binding of protons and metals by natural particulate matter (Lofts and Tipping, 1998). The code for the WHAM model incorporates a number of submodels: Humic Ion-Binding Model VI and a description of inorganic solution chemistry, cation exchange by clays, the precipitation of aluminium and iron oxyhydroxides, and adsorption-desorption of fulvic acids. The SCAMP model consists of three submodels: (1) Humic Ion-Binding Model VI, (2) a SCM describing proton and metal binding to oxides (i.e. AlOx , SiOx , MnOx and FeOx), and (3) a model describing the electrostatic exchange of cations on clays.

Model VI, a discrete binding site model in which binding is modified by electrostatic interactions, was described by Tipping (1998; 2002). It is worth noting that there is an empirical relationship between the net humic charge and an electrostatic interaction factor. The discrete binding sites are represented by two types of sites (A and B) and within each site type, there are four different sites present in equal amounts. The two types of sites are described by intrinsic proton binding constants (pK_A and pK_B) and spreads of the values (ΔpK_A and ΔpK_B) within each site type. There are n_A (mol g^{-1}) A-type sites (associated with carboxylic type groups) and $n_\text{B} = n_\text{A}/2$ (mol g^{-1}) B-type of sites (often associated with phenolic type groups). Metal binding occurs at single proton binding sites or by bidentate complexation between pairs of sites depending on a proximity factor that defines whether pairs of proton binding groups are close enough to form bidentate sites. Type A and Type B sites have separate intrinsic binding constants ($\log K_\text{MA}$ and $\log K_\text{MB}$), both of which are associated with a parameter, ΔLK_1 , defining the spread of values around the medians. A further parameter, ΔLK_2 , takes into account a small number of stronger sites. By considering results from many datasets, a universal average value of ΔLK_1 is obtained, and a correlation is established between $\log K_\text{MB}$ and $\log K_\text{MA}$ (Tipping, 1998). Then, a single adjustable parameter ($\log K_\text{MA}$) is necessary to fully describe the metal binding. The generic parameters for HA are presented in Table 1. WHAM 6 databases were modified by including $\log K_\text{MA}$ for V(IV)O complexation with fulvic and humic acids (Tipping, 2002) and well-accepted,

infinite dilution (25°C) stability constants for V(IV)O inorganic complexes (Wanty and Goldhaber, 1992 and references therein).

The SCAMP model (Lofts and Tipping, 1998) was also modified to include V species, as well as Fe, Mn and Al oxides. Briefly, SCAMP describes the equilibrium adsorption of protons and metals by natural particulate and colloidal matter using a combination of submodels for individual binding phases. Interactions with natural organic matter are described with Model VI, and adsorption by oxides with a surface complexation model that allows for site heterogeneity. An idealized cation exchanger is also included. SCAMP uses published parameters for Model VI, and the parameters for the oxide model are derived from published data for proton and metal binding by oxides of Al, Si, Mn, and Fe(III) (Table 2).

2.5 Data treatment

The ascending hierarchical classification using Ward's criterion was performed through XLSTAT so as to implement sample classification. This method is based on squared Euclidian distances between individuals in the space formed by the available variables. The initial sample is partitioned into several classes of individuals so as to maximize interclass inertia (i.e., to maximize variability between groups) and minimize intraclass inertia (i.e., to maximize homogeneity in each group). As for the factor analysis, the raw data matrix was introduced in the principal component analysis, without any rotation. The input data are the whole set of ultrafiltrates after each cut-off for all considered elements, as in Pourret et al. (2007b) and Pédrot et al. (2008).

3. Results

Measured concentrations of major and trace elements are reported in Table 3. The major and trace element data recovered after the filtration and ultrafiltration experiments will be discussed in the following section.

3.1 Temporal and spatial variation

The analytical data are reported in Table 3 and allow the recognition of two distinct groups of waters based on their spatial location. All data, except for V, have already been published elsewhere (Gruau et al., 2004).

3.1.1 Hillslope groundwaters

This first group - hillslope groundwater - corresponds to waters collected below the upland domain (P11 well) and below the upland–wetland transition zone (F5 and F7 wells). These waters display slightly acidic pH, low DOC, moderate to high NO_3^- concentrations, and low to very low REE, Th, U, Mn and Fe levels (Gruau et al., 2004; Table 3). Vanadium concentrations are also very low (Table 3). The most striking feature is the increasing V concentrations from upland to hillslope from $0.32 \mu\text{g L}^{-1}$ to $1.42 \mu\text{g L}^{-1}$. This spatial variation is followed by temporal variation from $0.35 \mu\text{g L}^{-1}$ to $0.78 \mu\text{g L}^{-1}$ and from $0.95 \mu\text{g L}^{-1}$ to $1.42 \mu\text{g L}^{-1}$ for the F5 and F7 wells, respectively.

3.1.2 Wetland groundwaters

The water samples of this group are restricted to wetland well F14 and have high to very high DOC contents (ranging from 7.98 mg L^{-1} to 53.10 mg L^{-1}), high REE, Th, U, Mn and Fe concentrations, and low to very low NO_3^- concentrations (Gruau et al., 2004). Vanadium

concentrations are also high and the range of V concentrations ($1.25 \mu\text{g L}^{-1}$ to $12.20 \mu\text{g L}^{-1}$) is large with values considerably higher than those reported for average world rivers ($0.76 \mu\text{g L}^{-1}$; Johannesson et al., 2000).

Systematic seasonal concentration changes are evidenced in these waters. As shown in Fig. 2, concentrations were rather low in January and increased markedly with the beginning of February until the middle of March, then showing an irregular decline from April to June 1999. Comparison of V data with Fe, Mn, DOC concentrations and redox potential results shows that the onset of V release at the end of January was concurrent with a decline of the redox potential (Fig. 2b, c) and coincides with an increase in DOC and both Mn and Fe concentrations (Figs. 2a, b, c and 3).

3.2 Ultrafiltration

In order to establish the role of organic colloids in the colourless, DOC-poor part of the *Le Home* water table and in DOC-rich water, hillslope and wetland groundwater samples (i.e., F7 and F14 wells) were successively filtered through membranes of smaller pore size (i.e., 30 kDa, 10 kDa and 5 kDa; see Table 4). Vanadium concentrations decrease upon successive filtrations at decreasing pore size (Figs. 5 and 6). These results illustrate differences with regards to the colloidal and dissolved partitioning of V in these two samples. Two clusters corresponding to common elemental distribution in the two samples were identified through the ascending hierarchical classification (Fig. 3), as following:

(i) cluster I: "truly" dissolved behaviour

Concentrations of Rb and alkaline metals such as Na and K are not affected by ultrafiltrations since no fractionation - following the decreasing pore sizes or the DOC concentrations - theoretically occurs. Alkaline elements behave as "truly" dissolved in the form of inorganic species as often reported in the literature (e.g., Pokrovsky and Schott, 2002). The

concentrations of major- and trace-alkaline metals (Ca, Mg, Rb, Sr and Ba) do not change significantly during filtration. Silica concentrations display no significant variations in the successive filtrates. This suggests that aqueous silica is not trapped by organic colloids and/or by small-size clay minerals or phytolites. Cobalt, Ni, Cr, Mn, Zn concentrations do not exhibit large variations through the different decreasing pore size cut-offs suggesting that these transition metals have to be mostly present as "truly" dissolved species or small size inorganic complexes (e.g., Gaillardet et al., 2003).

(ii) cluster II: colloidal pool-borne elements

Copper, REE, Pb, Th and U concentrations display extremely regular positive correlations versus DOC concentrations for both samples. The linear relationships (see Table 4) suggest that these trace elements are strongly bound to organic matter and probably complexed to very low molecular weight organic ligands such as extracellular ligands, as well as larger size colloids such as fulvic and/or humic acids, cell fragments or bacteria as elsewhere reported (e.g., Sigg et al., 2000; Pourret et al., 2007b). Aluminium and Fe concentration variations through successive filtrations suggest that: (i) these elements do not occur as free species in solution, and (ii) two types of colloids can carry these metals (i.e. Al-, Fe-rich inorganic colloids or organic-, Al-, Fe-complexing colloids). This indicates a major control of Al by inorganic mixed Fe/Al oxyhydroxides. Moreover, as shown in Pourret et al. (2007b), V displays an unpredictable behaviour with regards to the considered sample.

3.1.1 Hillslope groundwaters (F7)

Dissolved V was found to be associated with Fe colloids as their concentrations sharply decrease with decreasing pore size from 0.2 μm to 30 kDa (Fig. 5). It has been argued that dissolved V in rivers draining silicate rocks originates from silicate weathering (Shiller and Mao, 1999; Shiller and Mao, 2000). However, no correlation was observed between dissolved Si and V

in the studied samples. The presence of high amounts of colloidal Fe in these rivers, which serves as a potential V carrier, is likely to hide the different silicate vectors of V. The vanadium concentration displays a positive relationship with the DOC concentration, suggesting that the ability of V to form complexes with organic colloids remains constant over the molecular size range of the available colloid materials. The decrease following the lowering of the DOC concentrations suggests, on one hand, that for the uppermost sample, V is still carried by the organic phase (low- and high-molecular weight), and on the other hand, the decrease of V concentrations follows the same trend as that for Al. This suggests that V concentrations in such groundwater are controlled by mixed DOC/Al-rich phases, regardless of the pore size cut-off. Moreover, the large decrease of V concentrations following that of Fe between 0.2 μm and 30 kDa suggests, as earlier reported, that Fe-rich phases exert significant control on the speciation of V at this cut-off. At lower filtration sizes, V concentrations tend to be the lowest concentrations ($0.15 \mu\text{g L}^{-1}$), suggesting that V is also carried by a mixed Al/DOC-rich phase (Fig. 5).

3.2.2. Wetland groundwaters (F14)

Vanadium concentrations display a large drop between 0.2 μm and 30 kDa filtrations (Fig. 6), which may imply that a significant fraction (about 55%) of V is carried by large-size colloids. When looking at the lower cut-off data, the strong decrease in the first filtration step implies that V is strongly bound to high-molecular weight organic material. The nearly constant V concentration after the 30 kDa filtration implies that V behaves more independently of DOC (Fig. 6). Moreover, the V concentration pattern is different than that of the more DOC-depleted sample with far less variation regarding the Fe concentrations after 30 kDa filtration. This suggests that V should be partly carried by a Fe-rich phase. In addition, Fe concentrations strongly decrease with respect to the high molecular organic colloids (~80% in the > 30 kDa fraction) similarly to V, hence implying that V could be carried by mixed Fe-C phases.

Furthermore, when comparing the behaviour of V with respect to Al and Fe with that in the ultrafiltered DOC-depleted sample recovered from the hillslope (F7), we note that whereas V concentrations after the 30 kDa filtration follow the same trend as the Al and Fe concentrations in the wetland sample, V concentrations in the hillslope sample is mostly correlated with Al, but to a lesser extent with Fe. This latter point suggests that Fe and Al behave differently with regards to V in wetland and hillslope groundwater; low-molecular weight Fe compounds in the hillslope groundwater probably transport less V.

3.3 Speciation calculation using Model VI

Model VI and SCAMP included in WHAM 6.0 were used to calculate V speciation in groundwaters from the F7 and F14 wells. The modelling results were compared with the experimental data presented above. Major cations and anions were considered, as well as Fe and Al, for calculating the V speciation of the studied samples (see Table 4). In WHAM 6.0 (Lofts and Tipping, 1998), neither oxide precipitation nor redox reaction occur, so only complexation in solution is modelled by our speciation calculation. The assumption that 50% of the DOM is active as HM in our samples (Thurman, 1985), of which 80% is present as HA and 20% as FA (Viers et al., 1997), was chosen. More details on the "active" DOM parameter can be found in Pourret et al. (2007a; 2010). Aluminium colloids as well as Fe oxides were also considered (Lofts and Tipping, 1998). The speciation modelling results are displayed in Table 5.

Consistently with the ultrafiltration results, speciation calculations show that organic V species are the dominant species in the F7 groundwater (i.e., 47% complexed with HA and 47% with FA). The remaining V is present as $V(IV)O^{2+}$ (6%) (Table 5). In the F14 groundwater sample, the inorganic proportion of V is lower (i.e., only 1%). Speciation calculations show that organic V species are also the dominant species in the F14 groundwater (i.e., 58% complexed with HA and 41% with FA) (Table 5). Therefore, as with the ultrafiltration results, the speciation

modelling calculations illustrate a slight change of the V speciation in groundwaters along the *Le Home* transect. Vanadium in the hillslope groundwaters wells occurs as a mixing of organic and inorganic complexes, whereas V in the wetland groundwaters wells comprises mainly organic species. It is worth to underline that the modelling calculation and ultrafiltration results both conclude that the downhill decrease in inorganic complexation occurs in phase with a progressive scavenging of the V by a colloidal organic pool.

4. Discussion

4.1 Approach limitation

The authors of the WHAM-SCAMP model have noted a number of possible pitfalls in its application (Lofts and Tipping, 1998); the major ones are as follows: (i) the application of the WHAM-SCAMP model relies upon consistency between the metal binding data obtained for laboratory prepared phases and the metal binding properties of component phases found in natural colloidal assemblages; (ii) the surface complexation modelling technique is difficult to adapt in order to obtain model parameters from experimental Mn oxide data available in the literature (e.g., Dzombak and Morel, 1990; Kosmulski, 2006); (iii) there is some evidence in the literature that component phases constituting natural particulate materials are intimately associated (Peacock and Sherman, 2004); and (iv) ternary surface complexes are not considered even if it has been shown that Fe-rich organic colloids may adsorb metal ions (Buffle et al., 1998; Fein, 2002; Hiemstra and Van Riemsdijk, 1999; Schindler, 1990). These types of associations have implications when considering the validity of the modelling approach, which relies upon the assumption that the components of the colloidal assemblage exist as discrete phases. Lofts and Tipping (1998) note that these associations can lead to a deviation from the additivity of metal

binding expected from a simple combination of isolated phases such as DOC-rich colloids, and Mn and Fe oxyhydroxides.

Vanadium(IV) may account for more than 50% of the total dissolved V in mildly reducing groundwaters (Bosque-Sendra et al., 1998; Elbaz-Poulichet et al., 1997; Emerson and Husted, 1991). Both the oxidation rate from V(IV) to V(V) and the coexistence of the two species in aqueous solution depend on the pH, V concentration, reduction-oxidation potential and ionic strength of the system (Fig. 7). Even if V(IV) is not thermodynamically stable above pH 7, complexation by various organic and inorganic species may considerably increase its stability (Lu et al., 1998; Szalay and Szilagyi, 1967; Tribovillard et al., 2006; Wanty and Goldhaber, 1992). Thus, V(IV) has only been considered in a speciation calculation performed using the WHAM-SCAMP model, considering a pH below 7 and DOC concentrations ranging between 11.1 and 21.5 mg L⁻¹.

Although the 5 kDa cut-off allows very small size colloids to remain in solution, the lack of integration of adsorption processes onto inorganic species, as well as the coprecipitation of inorganic species appear to be the major causes of divergence between ultrafiltration data and speciation calculations for V. It is then important to be aware that this type of model does not take into account any uptake of metals resulting from competitive reactions between Fe-rich and DOC-rich colloids and that the occurrence of ternary surface complexes is thus not considered.

The studied samples are organic-rich groundwaters with an organic pool that seems to be in excess with regards to the metals available for complexation. However, this kind of competition (i.e., ternary surface complexes) is still difficult to interpret using only ultrafiltration data. Cation ligand complexes can be adsorbed onto solid particles to form ternary surface complexes either as a cation linked to the mineral surface over the ligand or as a ligand linked to the surface over the cation (Buerge-Weirich et al., 2002). As an example, relatively recently published data on REE (Davranche et al., 2008) showed the impact of ternary surface complexes (humates/oxyhydroxides/REE) on metal speciation. Thus, it appears necessary for speciation

models to take processes such as adsorption onto Mn and Fe oxyhydroxides into account - considering that the lack of such a reaction precludes any true speciation to be assessed - as the competition between Fe and C-based colloidal carriers is required for constraining element geochemical cycles or element fate in polluted environments. Apart from this, such a modelling approach is not intrinsically incorrect (Zhu and Anderson, 2002); these values may well be the best possible overall values even if they cannot be extrapolated to all applications.

4.2 Colloid-mediated control on V distribution in shallow groundwaters

It is now widely accepted that the colloidal phase plays a significant role in the transport and cycling of trace metals in water as assessed here for V, as it has already been illustrated for REE on this catchment (Gruau et al., 2004; Pourret et al., 2007a). Colloid-mediated carriage of V has been well described (Dupré et al., 1999; Gaillardet et al., 2003; Lyvén et al., 2003; Pokrovsky et al., 2005; 2006; Dahlgqvist et al., 2007; Pourret et al., 2007b; Pédrot et al., 2008; 2009), although not unambiguously with regards to the nature and source of the involved V carrier phases, as often debated elsewhere (e.g., Lyvén et al., 2003 and references therein). Key issues still have to be answered such as: which role is played by (i) the source-rock, (ii) the organic matter, (iii) the true competition between Fe- and C-based colloidal carriers for V, and whether or not the colloidal pool involved in V carriage in solution be typed.

4.2.1 Influence of source-rock on vanadium speciation in solution

Since the fraction of dissolved V has been shown to be primarily derived from silicates with an efficiency comparable to that of dissolved silicate during weathering, chemical weathering of silicate rocks has been considered as the primary control of the globally encountered dissolved V (Shiller and Mao, 2000; Wright and Belitz, 2010). Elbaz-Poulichet et al.

(1997) proposed that alumina-silicate colloids are a dominant host for V in water. However, V-focused studies emphasized that silicate weathering cannot be the only controlling speciation with regards to V dissolved species. The so-called ‘secondary factors’, as referred by Shiller and Mao (2000), include the nature, style and regime of the prevailing weathering processes (Gaillardet et al., 2003), redox reactions, organic-mediated complexation and anthropogenic inputs. Furthermore, Wehrli and Stumm (1989) considered that VO^{2+} has a strong tendency to coordinate with oxygen donor atoms, thus forming both strong complexes with organic chelates and becoming adsorbed especially onto hydrous oxides. Vanadium(V) - as vanadate oxyanion - behaves as phosphate and forms surface complexes with hydrous oxides by ligand exchange. These results led us to the assumption that, although not excluding a primary source of V in silicate weathering, the V stock available in wetland soil solutions mostly results from surface processes at organic matter/solution/hydrous oxide interfaces probably driven by acid-base and redox reactions. Moreover, as also stressed by Pokrovsky and Schott (2002) who did not find any relationships between V and Si in the Karelian rivers, no correlation was observed between dissolved V and Si, irrespective of the pore size cut-off used for ultrafiltration (Tables 2 and 3). Hence, dissolved V behaves independently of dissolved Si. The occurrence of large amounts of colloidal Fe and/or C that serve as efficient V carriers as assessed by the positive relationships between DOC and V as well as Fe and V (Figs. 5 and 6), as has often been previously reported, is likely to hide the fingerprint of the source-rock of V. Two studies by Dupré et al. (1999) and Pokrovsky and Schott (2002) reached the same conclusion. In the first case, these authors observed that V content and DOC decrease during successive filtrations through decreasing pore size membranes, whereas in the latter study, the dissolved V was found to be essentially associated with the Fe colloids, as their concentrations sharply decrease with decreasing pore size. The presence of high amounts of colloidal Fe or C in these rivers, which serve as a V carrier, is thus likely to hide the different silicate sources.

4.2.2 Influence of the colloid type in the transport of vanadium

Since the source rocks do not reflect the major control of dissolved V speciation and considering that it is now widely admitted that colloids are major V carriers playing a significant role in both the transport and cycling of V in natural waters, the question becomes which is the prevailing nature of the colloidal carriers of V. The above discussion, with regards to the role played by the source-rocks, showed a different behaviour to that proposed by Elbaz-Poulichet et al. (1997) for the silica-rich colloids, except for very specific cases.

On one side, the observed time-linked variations showed that the onset of V in solution at the end of January and following the decline of redox potential (Fig. 2b) occurred concomitantly with the increase of DOC, Mn and Fe concentrations (Figs. 2 and 3). Nevertheless, it is not possible to assess which of the metallic or organic phases could be the most efficient V carrier. On the other side, when considering the space-linked variations, the increase of V concentrations from upland (P11) to hillslope (F5-F7), as seen in the DOC concentrations, were observed, thereby suggesting that V might be carried by C-rich phases, as also found in other studies (Wehrli and Stumm, 1989; Dupré et al., 1999; Tyler, 2004; Audry et al., 2006). This feature has already been observed for REE whose speciation is considered as being mostly organic (Gruau et al., 2004; Pourret et al., 2007b). Indeed, the largest V concentrations are observed for wetland well F14, reaching up to 12.2 mg L⁻¹ (Table 3). However, these concentrations also follow both the highest DOC and Fe contents, making it impossible to unambiguously determine whether the C- or Fe-colloids are the most efficient V carriers. Therefore, neither time-linked V nor space-linked concentration variations, in both cases positively related to the DOC and Fe variations, allowed to distinguish between the predominance of C-or Fe-colloidal carrying phases. However, Pourret et al. (2007a) suggested that the “colloidal” REE budget of samples F7 and F14 is partly controlled by REE-bearing Fe colloids and the contribution of Fe colloids estimated between ~30 and 50%.

Further information can be obtained from ultrafiltration data on hillslope and wetland samples as has been done in a previous study (Pourret et al., 2007b). The ascending hierarchical classification displayed in Figure 3 reveals - beyond the first evidence that V is mostly borne by the colloidal pool since its concentrations decrease following decreasing pore size cut-off - that the hillslope groundwater sample F7 shows a double control of V distribution by large-size (0.2 μm and 30 kDa) Fe-rich colloids, as reported by Pédrot et al. (2009). A continuous control by a mixed DOC/Al-rich phase is also simultaneously seen, irrespective of the size of the concerned colloidal pool (Fig. 5). This control by the mixed DOC/Al-rich phase has been also already shown elsewhere, but in a similar context by Pourret et al. (2007b), who showed that concentrations of both dissolved V and Th were mostly controlled by mixed DOC/Al-rich phases, regardless of the filtration membrane cut-off. In the hillslope case, V is therefore carried on one side by the large-size (> 30 kDa) Fe oxide colloidal phase and mixed DOC/Al-rich phases (Fig. 5).

Although large-size Fe colloids are also involved in V dissolved carriage, the coupled observation of Fig. 3 and Fig. 5 led to the assumption that the major colloidal control for maintaining V in dissolved phase has to be mixed DOC/Al phases since V distribution appears closer to those of DOC and Al than to that of Fe (Fig. 3). Additionally, the V versus DOC and Al distribution (Fig. 5) displays a positive relationship, regardless of the size cut-off, whereas Fe is not carried by DOC-rich low-molecular weight colloids still carrying V. This has to be compared to previous studies such as the one carried out by Pokrovsky et al. (2006), who observed that V did not exhibit any clear correlation with dissolved Fe or DOC in the < 0.2 μm fraction. By contrast, ultrafiltration performed on peat solution showed that Al played an important role as a colloidal carrier of V (Pokrovsky et al., 2005). In another context, field-flow fractionation performed on freshwaters showed that V was strongly associated to iron-rich colloids (Stolpe et al., 2005).

Another interesting point is that the observed V concentrations are also much higher than those reported for average world rivers (Johannesson et al., 2000) (Fig. 7) suggesting that the involved mixed DOC/Al colloidal carriers of V emphasize the level of dissolved V in such organic-rich environments, possibly, as proposed by Wehrli and Stumm (1989), as complexes with humic substances (HS) (Tyler, 2004) in which Al, V and HS are intimately associated. This has to be related to the fact that VO^{2+} is commonly considered as an exceptionally stable diatomic ion (Greenwood and Earnshaw, 1997), which forms strong complexes with soluble organic compounds (Aström and Corin, 2000). Such speciation information must also be linked with the sequential extraction experiments conducted on soil samples such as those of Poledniok and Buhl (2003) showing that V is mainly contained in the organic fractions.

The observation of Figure 6, corresponding to the sample recovered in the wetland (F14), led to a slightly different result, although characterized by an important combined Al/DOC control on the V distribution. In this case, the Fe distribution follows that of V throughout the pore size cuts, which was not the case for the hillslope sample (F7) which displayed a drastic fall between 0.2 μm and 30 kDa, pointing out a non-exclusively organic speciation. Ultrafiltration data on the wetland sample (F14) point out a triple control of mixed Fe/Al/C-rich carrier phases of V, which may correspond to nano-colloidal Fe oxides embedded within Al-enriched humic substances, as elsewhere evidenced in wetlands and experimentally shown to be a significant source of bioavailable Fe (Pédrot et al., 2011). Such colloid-mediated organically complexed V is probably transported by humic substances from the source areas located in the humus-rich uppermost horizons.

Therefore, V speciation changes between the hillslope and the wetland, as assessed from the ultrafiltration data, agree with modelling calculations. Vanadium carriage moves from (i) the hillslope with a shared contribution of Fe nanooxide and organic colloids vector towards (ii) the wetland with a whole organic pool in which V, Fe and Al are complexed and embedded in organic matrices. This is also often pointed out for other trace metals elsewhere in wetlands (e.g.,

Gruau et al., 2004), whose interaction with mineral colloids is hampered by the negative charge of organic matter (i.e., Wilkinson et al., 1997), which is ubiquitous in such waterlogged environments.

5. Conclusions

Combining an ultrafiltration fractionation approach and modelling conducted on shallow groundwaters allowed the assessment of the main factors that control V speciation. Additionally, it can be concluded that the water samples can be divided into two groups in terms of their location along the hillslope and their associated DOC content, which are positively related to their V content (organic-rich waters recovered in wetland display the largest V concentrations). Moreover, time variations of V concentrations were also seen in wetland samples with a marked increase of V content at the winter-spring transition along with DOC, Fe and Mn content variations, as well as redox potential changes. In this context, the source rock was shown to play a minor role in V distribution, whereas the colloidal pool was shown to be the main factor controlling V speciation and its distribution in shallow groundwaters. Ascendant hierarchical classification showed that V was associated to DOC, Fe, Al, Pb, Cu, REE, U and Th, which are elements known to exhibit colloidal affinity. Speciation modelling using Model VI and SCAMP as well as ultrafiltration data evidenced a slight change in the V speciation occurring along the transect with a mixed organic-inorganic speciation in the hillslope and an organic speciation of V in the wetland probably involving Fe nanooxides embedded in Al-rich organic colloids. The binding of V in this organic environment most likely occurs through the C-rich ligand end-member, which is in agreement with the behaviour of V in shallow groundwater.

Although the role of organic matter is clearly assessed as controlling the dissolved V fraction, it appears challenging to accurately determine the real contribution of the inorganic and organic colloidal pool because the oxides are generally intimately bound to the organic matter,

621 especially in the case of organic-rich wetland soil solutions. Further study should be dedicated to
622 clarifying this partition, notably to address the prevailing processes affecting V transport at the
623 global scale.

624

625 **Acknowledgements**

626 The authors thank O. Hénin and P. Petitjean for their assistance during the sampling and
627 analytical work, Dr. P. Jitaru for insightful comments, and Dr S. Mullin for post-editing the
628 English style.

629

- 631
632 Åström, M., Corin, N., 2000. Abundance, sources and speciation of trace elements in humus-rich
633 streams affected by acid sulphate soils. *Aquatic Geochemistry*, 6, 367-383.
- 634 Audry, S., Blanc, G., Schäfer, J., Chaillou, G., Robert, S., 2006. Early diagenesis of trace metals
635 (Cd, Cu, Co, Ni, U, Mo, and V) in the freshwater reaches of a macrotidal estuary.
636 *Geochimica et Cosmochimica Acta*, 70, 2264-2282.
- 637 Bosque-Sendra, J.M., Valencia, M.C., Boudra, S., 1998. Speciation of vanadium (IV) and
638 vanadium (V) with Eriochrome Cyanine R in natural waters by solid phase
639 spectrophotometry. *Fresenius' Journal of Analytical Chemistry*, 360, 31-37.
- 640 Bouhnik-Le Coz, M., Petitjean, P., Serrat, E., Gruau, G., 2001. Validation d'un protocole
641 permettant le dosage simultané des cations majeurs et traces dans les eaux douces
642 naturelles par ICP-MS, *Cahiers Techniques*, 1. Géosciences Rennes, Rennes, France, 77
643 pp. Available at: http://www.geosciences.univ-rennes1.fr/IMG/pdf/Cahier_n1.pdf.
- 644 Breit, G.N., Wanty, R.B., 1991. Vanadium accumulation in carbonaceous rocks: a review of
645 geochemical controls during deposition and diagenesis. *Chemical Geology*, 91, 83-97.
- 646 Buerge-Weirich, D., Hari, R., Xue, H., Behra, P., Sigg, L., 2002. Adsorption of Cu, Cd, and Ni
647 on goethite in the presence of natural groundwater ligands. *Environmental Science &*
648 *Technology*, 36, 328-336.
- 649 Buffle, J., Wilkinson, K., Stoll, S., Filella, M., Zhang, J., 1998. A generalized description of
650 aquatic colloidal interactions: the three-colloidal component approach. *Environmental*
651 *Science & Technology*, 32, 2887-2899.
- 652 Calvert, S.E., Pedersen, T.F., 1993. Geochemistry of recent oxic and anoxic marine sediments:
653 Implication for the geological record. *Marine Geology*, 113, 67-88.
- 654 Clément, J.-C., Aquilina, L., Bour, O., Plaine, K., Burt, T.P., Pinay, G., 2003. Hydrological
655 flowpaths and nitrate removal rates within a riparian floodplain along a fourth-order
656 stream in Brittany (France). *Hydrological Processes*, 17, 1177-1195.
- 657 Dahlqvist, R., Andersson, K., Ingri, J., Larsson, T., Stolpe, B., Turner, D., 2007. Temporal
658 variations of colloidal carrier phases and associated trace elements in a boreal river.
659 *Geochimica et Cosmochimica Acta*, 71, 5339-5354.
- 660 Davranche, M., Pourret, O., Gruau, G., Dia, A., Jin, D., Gaertner, D., 2008. Competitive binding
661 of REE to humic acid and manganese oxide: impact of reaction kinetics on development
662 of Cerium anomaly and REE adsorption. *Chemical Geology*, 247, 154-170.
- 663 Dupré, B., Viers, J., Dandurand, J.-L., Polvé, M., Bénézech, P., Vervier, P., Braun, J.-J., 1999.
664 Major and trace elements associated with colloids in organic-rich river waters:
665 ultrafiltration of natural and spiked solutions. *Chemical Geology*, 160, 63-80.
- 666 Dzombak, D.A., Morel, F.M.M., 1990. Surface complexation modeling-hydrous ferric oxide.
667 Wiley, New York, 393 pp.
- 668 Elbaz-Poulichet, F., Nagy, A., Cserny, T., 1997. The distribution of redox sensitive elements (U,
669 As, Sb, V and Mo) along a river-wetland-lake system (Balaton Region, Hungary).
670 *Aquatic Geochemistry*, 3, 267-282.
- 671 Emerson, S.R., Huested, S.S., 1991. Ocean anoxia and the concentrations of molybdenum and
672 vanadium in seawater. *Marine Chemistry*, 34, 177-196.
- 673 Fein, J.B., 2002. The effects of ternary surface complexes on the adsorption of metal cations and
674 organic acids onto mineral surfaces. In: R. Hellmann and S.A. Wood (Editors), *Water-*
675 *Rock Interactions, Ore Deposits, and Environmental Geochemistry: A Tribute to David*
676 *A. Crerar*. Geochemical Society, Special Pub. 7, pp. 365-378.
- 677 Francois, R., 1988. A study on the regulation of the concentrations of some trace metals (Rb, Sr,
678 Zn, Pb, Cu, V, Ni, Mn and Mo) in Saanich Inlet sediments, British Columbia, Canada.
679 *Marine Geology*, 83, 285-308.

- Gaillardet, J., Viers, J., Dupré, B., 2003. Trace Elements in River Waters. In: E.D. Holland, Turekian, K.K. (Editor), *Treatise on Geochemistry*. Elsevier-Pergamon, pp. 225-263.
- Greenwood, N.N., Earnshaw, A., 1997. *Chemistry of the Elements*. Butterworth-Heinemann, Oxford, 1600 pp.
- Gruau, G., Dia, A., Olivie-Lauquet, G., Davranche, M., Pinay, G., 2004. Controls on the distribution of rare earth elements in shallow groundwaters. *Water Research*, 38, 3576-3586.
- Hastings, D.W., Emerson, S.R., Erez, J., Nelson, B.K., 1996. Vanadium in foraminiferal calcite: Evaluation of a method to determine paleo-seawater vanadium concentrations. *Geochimica et Cosmochimica Acta*, 60, 3701-3715.
- Hiemstra, T., Van Riemsdijk, W.H., 1999. Surface structural ion adsorption modeling of competitive binding of oxyanions by metal (hydr)oxides. *Journal of Colloid and Interface Science*, 210, 182-193.
- Hope, B.K., 1997. An assessment of the global impact of anthropogenic vanadium. *Biogeochemistry*, 37, 1-13.
- Hope, B.K., 2008. A dynamic model for the global cycling of anthropogenic vanadium. *Global Biogeochemical Cycles*, 22, GB4021.
- Johannesson, K.H., Lyons, W.B., Graham, E.Y., Welch, K.A., 2000. Oxyanion concentrations in eastern Sierra Nevada rivers - 3. Boron, molybdenum, vanadium, and tungsten. *Aquatic Geochemistry*, 6, 19-46.
- Kosmulski, M., 2006. pH-dependent surface charging and points of zero charge III. Update. *Journal of Colloid and Interface Science*, 298, 730-741.
- Lofts, S., Tipping, E., 1998. An assemblage model for cation binding by natural particulate matter. *Geochimica et Cosmochimica Acta*, 62, 2609-2625.
- Lowenthal, D.H., Borys, R.D., Chow, J.C., Rogers, F., 1992. Evidence for long-range transport of aerosol from the Kuwaiti Oil fires to Hawaii. *Journal of Geophysical Research*, 97, 14,573-14,580.
- Lu, X., Johnson, W.D., Hook, J., 1998. Reaction of vanadate with aquatic humic substances: An ESR and 51V NMR study. *Environmental Science & Technology*, 32, 2257-2263.
- Lyvén, B., Hasselöv, M., Turner, D.R., Haraldsson, C., Andersson, K., 2003. Competition between iron- and carbon-based colloidal carriers for trace metals in a freshwater assessed using flow field-flow fractionation coupled to ICPMS. *Geochimica et Cosmochimica Acta*, 67, 3791-3802.
- Moskalyk, R.R., Alfanti, A.M., 2003. Processing of vanadium: a review. *Minerals Engineering*, 16, 793-805.
- Peacock, C.L., Sherman, D.M., 2004. Vanadium(V) adsorption onto goethite (α -FeOOH) at pH 1.5 to 12: A surface complexation model based on ab initio molecular geometries and EXAFS spectroscopy. *Geochimica et Cosmochimica Acta*, 68, 1723-1733.
- Pédrot, M., Dia, A., Davranche, M., Bouhnik-Le Coz, M., Henin, O., Gruau, G., 2008. Insights into colloid-mediated trace element release at the soil/water interface. *Journal of Colloid and Interface Science*, 325, 187-197.
- Pédrot, M., Dia, A., Davranche, M., 2009. Double pH control on humic substance-borne trace elements distribution in soil waters as inferred from ultrafiltration. *Journal of Colloid and Interface Science*, 339, 390-403.
- Pédrot, M., Le Boudec, A., Davranche, M., Dia, A. and Henin, O., 2011. How does organic matter constrain the nature, size and availability of Fe nanoparticles for biological reduction? *Journal of Colloid and Interface Science*, 359: 75-85.
- Petitjean, P., Henin, O., Gruau, G., 2004. Dosage du carbone organique dissous dans les eaux naturelles. Intérêt, principe, mise en oeuvre et précautions opératoires. *Cahiers Techniques*, 3. Géosciences Rennes, Rennes, France, 64 pp. Available at: http://www.geosciences.univ-rennes1.fr/IMG/pdf/Cahier_n3.pdf.

- 731 Pokrovsky, O.S., Schott, J., 2002. Iron colloids/organic matter associated transport of major and
 732 trace elements in small boreal rivers and their estuaries (NW Russia). *Chemical Geology*,
 733 190, 141-179.
- 734 Pokrovsky, O.S., Dupré, B., Schott, J., 2005. Fe-Al-organic colloids control of trace elements in
 735 peat soil solutions: results of ultrafiltration and dialysis. *Aquatic Geochemistry*, 11, 241-
 736 278.
- 737 Pokrovsky, O.S., Schott, J., Dupré, B., 2006. Trace element fractionation and transport in boreal
 738 rivers and soil porewaters of permafrost-dominated basaltic terrain in Central Siberia.
 739 *Geochimica et Cosmochimica Acta*, 70, 3239-3260.
- 740 Poledniok, J., Buhl, F., 2003. Speciation of vanadium in soil. *Talanta*, 59, 1-8.
- 741 Pourret, O., Davranche, M., Gruau, G., Dia, A., 2007a. Organic complexation of rare earth
 742 elements in natural waters: Evaluating model calculations from ultrafiltration data.
 743 *Geochimica et Cosmochimica Acta*, 71, 2718-2735.
- 744 Pourret, O., Dia, A., Davranche, M., Gruau, G., Hénin, O., Angée, M., 2007b. Organo-colloidal
 745 control on major- and trace-element partitioning in shallow groundwaters: confronting
 746 ultrafiltration and modelling. *Applied Geochemistry*, 22, 1568-1582.
- 747 Pourret, O., Gruau, G., Dia, A., Davranche, M., Molénat, J., 2010. Colloidal control on the
 748 distribution of rare earth elements in shallow groundwaters. *Aquatic Geochemistry*, 16,
 749 31-59.
- 750 Rühling, A., Tyler, G., 2001. Changes in atmospheric deposition rates of heavy metals in
 751 Sweden. *A summary of Nationwide Swedish Surveys in 1968/70-1995*. Water, Air, and
 752 Soil Pollution: Focus, 1, 311-323.
- 753 Schindler, P.W., 1990. Co-adsorption of metal ions and organic ligands: formation of ternary
 754 surface complexes. In: M.F. Hochella and A.F. White (Editors), *Mineral-Water Interface*
 755 *Geochemistry*. Mineralogical Society of America, pp. 281-307.
- 756 Seyler, P.T., Boaventura, G.R., 2003. Distribution and partition of trace metals in the Amazon
 757 basin. *Hydrological Processes*, 17, 1345-1361.
- 758 Shiller, A.M., 1997. Dissolved trace elements in the Mississippi River: Seasonal, interannual, and
 759 decadal variability. *Geochimica et Cosmochimica Acta*, 61, 4321-4330.
- 760 Shiller, A.M., Boyle, E.A., 1987. Dissolved vanadium in rivers and estuaries. *Earth and Planetary*
 761 *Science Letters*, 86, 214-224.
- 762 Shiller, A.M., Mao, L., 1999. Dissolved vanadium on the Louisiana Shelf: effect of oxygen
 763 depletion. *Continental Shelf Research*, 19, 1007-1020.
- 764 Shiller, A.M., Mao, L., 2000. Dissolved vanadium in rivers: effect of silicate weathering.
 765 *Chemical Geology*, 165, 13-22.
- 766 Sugiyama, M., 1989. Seasonal variation of vanadium concentration in Lake Biwa, Japan.
 767 *Geochemical Journal*, 23, 111-116.
- 768 Stolpe, B., Hassellöv, M., Anderson, K., Turner, D.R., 2005. High resolution ICPMS as an on-
 769 line detector for flow field-flow fractionation: multi-element determination of colloidal
 770 size distributions in a natural water sample. *Analytica Chimica Acta*, 535, 109-121.
- 771 Szalay, A., Szilagyi, M., 1967. The association of vanadium with humic acids. *Geochimica et*
 772 *Cosmochimica Acta*, 31, 1-6.
- 773 Takahashi, Y., Minai, Y., Ambe, S., Makide, Y., Ambe, F., Tominaga, T., 1997. Simultaneous
 774 determination of stability constants of humate complexes with various metal ions using
 775 multitracer technique. *Science of the Total Environment*, 198, 61-71.
- 776 Templeton, G.D., Chasteen, N.D., 1980. Vanadium-fulvic acid chemistry: conformational and
 777 binding studies by electron spin probe techniques. *Geochimica et Cosmochimica Acta*,
 778 44, 741-752.
- 779 Thurman, E.M., 1985. *Organic Geochemistry of Natural Waters*. Kluwer, Dordrecht, 497 pp.

- Tipping, E., 1994. WHAM - A chemical equilibrium model and computer code for waters, sediments, and soils incorporating a discrete site/electrostatic model of ion-binding by humic substances. *Computers & Geosciences*, 20, 973-1023.
- Tipping, E., 1998. Humic Ion-Binding Model VI: an improved description of the interactions of protons and metal ions with humic substances. *Aquatic Geochemistry*, 4, 3-48.
- Tipping, E., 2002. Cation binding by humic substances. University Press, Cambridge, 434 pp.
- Tribovillard, N., Algeo, T.J., Lyons, T., Riboulleau, A., 2006. Trace metals as paleoredox and paleoproductivity proxies: An update. *Chemical Geology*, 232, 12-32.
- Tyler, G., 2004. Vertical distribution of major, minor, and rare elements in a Haplic Podzol. *Geoderma*, 119, 277-290.
- Viers, J., Dupré, B., Polvé, M., Schott, J., Dandurand, J.-L., Braun, J.J., 1997. Chemical weathering in the drainage basin of a tropical watershed (Nsimi-Zoetele site, Cameroon): comparison between organic-poor and organic-rich waters. *Chemical Geology*, 140, 181-206.
- Wang, D., Sanudo Wilhelmy, S.A., 2009. Vanadium speciation and cycling in coastal waters. *Marine Chemistry*, 117, 52-58.
- Wanty, R.B., Goldhaber, M.B., 1992. Thermodynamics and kinetics of reactions involving vanadium in natural systems: accumulation of vanadium in sedimentary rocks. *Geochimica et Cosmochimica Acta*, 56, 1471-1483.
- Wehrli, B., Stumm, W., 1989. Vanadyl in natural waters: Adsorption and hydrolysis promote oxygenation. *Geochimica et Cosmochimica Acta*, 53, 69-77.
- Wilkinson, K.J., Nègre, J.-C., Buffle, J., 1997. Coagulation of colloidal material in surface waters: the role of natural organic matter. *Journal of Contaminant Hydrology*, 26, 229-243.
- Wright, M.T., Belitz, K., 2010. Factors controlling the regional distribution of vanadium in groundwater. *Ground Water*, 48, 515-525.
- Yeghicheyan, D., Carignan, J., Valladon, M., Bouhnik Le Coz, M., Le Cornec, F., Castrec-Rouelle, M., Robert, M., Aquilina, L., Aubry, E., Churlaud, C., Dia, A., Deberdt, S., Dupré, B., Freydier, R., Gruau, G., Hénin, O., de Kersabiec, A.-M., Macé, J., Marin, L., Morin, N., Petitjean, P., Serrat, E., 2001. Compilation of silicon and thirty one trace elements measured in the natural river water reference material SLRS-4 (NRC-CNRC). *Geostandards Newsletter*, 25, 465-474.
- Zhu, C., Anderson, G., 2002. Environmental Applications of Geochemical Modeling. University Press, Cambridge, 284 pp.

816 TABLE AND FIGURE CAPTIONS
817

818 Table 1. Model VI parameters for humic substances (Tipping, 1998; Tipping, 2002).

819

820 Table 2. SCAMP parameter values for Fe, Mn, Al and Si oxide. Site density Γ_{\max} is expressed in
821 $\mu\text{mol m}^{-2}$ and P in $\text{m}^2 \text{eq}^{-1}$ (data are from Lofts and Tipping, 1998). Values of pK_{MH} for V(IV)O
822 are calculated from Eqns. 10 to 13 in Lofts and Tipping (1998) using well-accepted infinite-
823 dilution (25°C) stability constants for V(IV)O first hydrolysis complexes (Peacock and Sherman,
824 2004).

825

826 Table 3. Physico-chemical parameters: pH, Eh (in mV) and temperature (in °C), and chemical
827 concentrations ($\mu\text{g L}^{-1}$), except for Cl^- , NO_3^- , SO_4^{2-} and DOC, which are reported in mg L^{-1} .

828

829 Table 4. Ultrafiltration results; the concentrations are expressed in $\mu\text{g L}^{-1}$, except for Cl^- , NO_3^-
830 SO_4^{2-} and DOC which are reported in mg L^{-1} , and alkalinity in $\mu\text{mol L}^{-1}$.

831

832 Table 5. Speciation results obtained using Model VI and SCAMP for groundwater from the F7
833 and F14 wells (species proportion).

834

835 Figure 1. Geographical location of the Petit Hermitage Catchment (France) and well water
836 sampling placements set up along the *Le Home* toposequence.

837

838 Figure 2. Time series results of dissolved ($< 0.2 \mu\text{m}$) (a) Fe and Mn (mg L^{-1}), (b) V and U ($\mu\text{g L}^{-1}$)
839 and (c) Eh (mV) and DOC (mg L^{-1}) content in the *Le Home* wetland samples (F14 well).

840

Figure 3. Dendograms of samples (a) F7 and (b) F14, showing the hierarchical classification of the elements in three clusters.

Figure 4. Relationships between: (a) V and DOC and (b) V and Fe concentrations for the F14 groundwater samples. The data are expressed in mg L^{-1} except for V ($\mu\text{g L}^{-1}$). The corresponding values are provided in Table 3.

Figure 5. Variations of (a) V and Al versus DOC concentrations and (b) V and Fe versus DOC concentrations in the different filtrates for the F7 well. The corresponding values are provided in Table 4.

Figure 6. Variations of (a) V and Al versus DOC concentrations and (b) V and Fe versus DOC concentrations in the different filtrates for the F14 well. The corresponding values are provided in Table 4.

Figure 7. Eh/pH diagram for inorganic V species at 25°C and 1 atm for a V concentration of $10 \mu\text{mol L}^{-1}$ (Breit and Wanty, 1991; Peacock and Sherman, 2004; Templeton and Chasteen, 1980; Wanty and Goldhaber, 1992; Wehrli and Stumm, 1989). Vanadium data (black dots) are from Table 2.

Figure 1

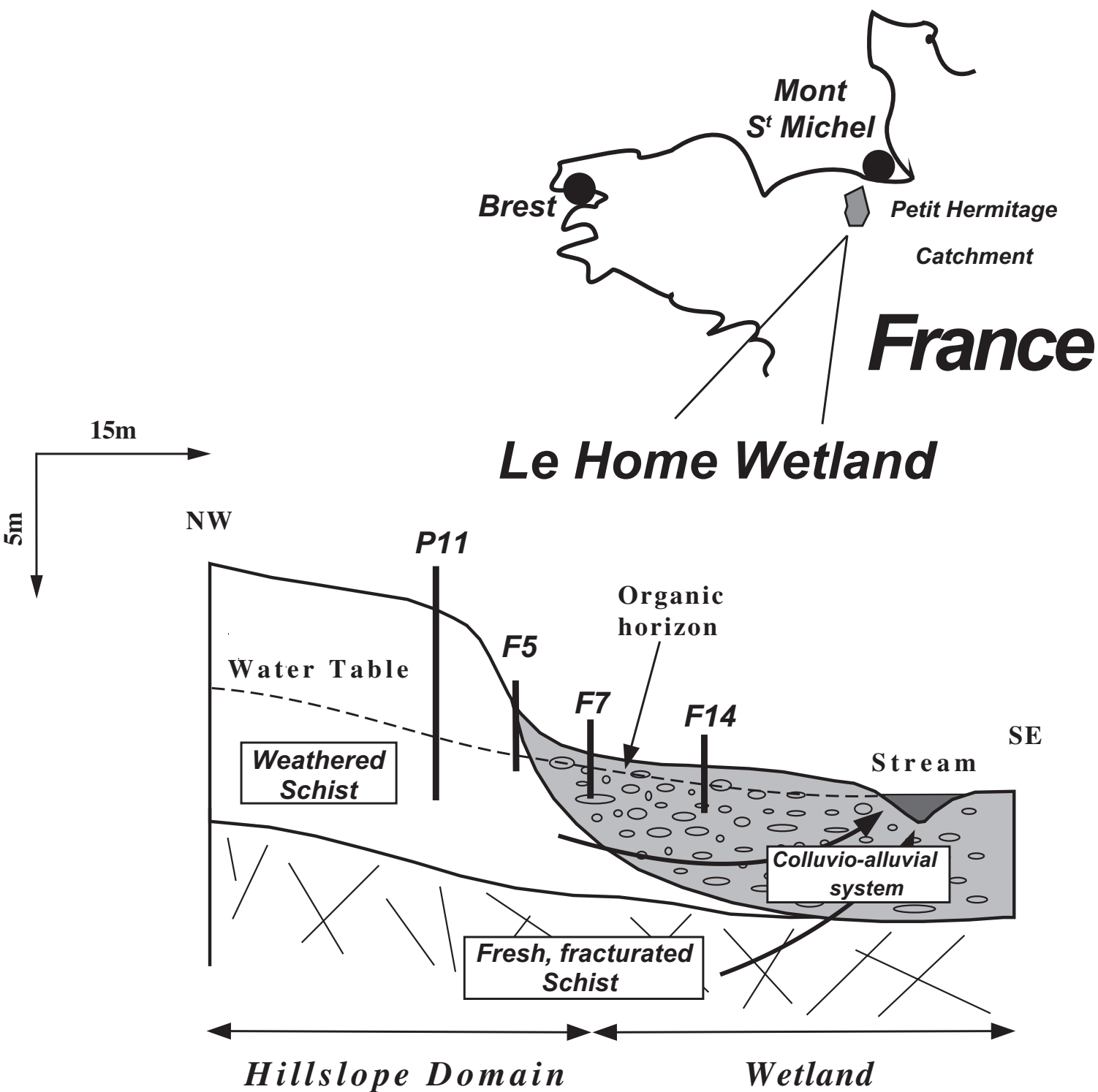


Figure 2

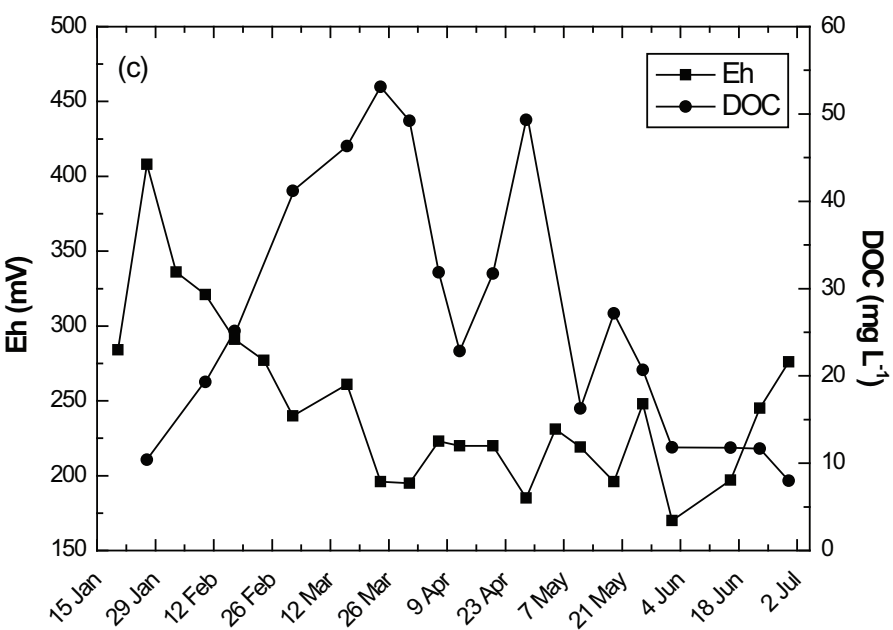
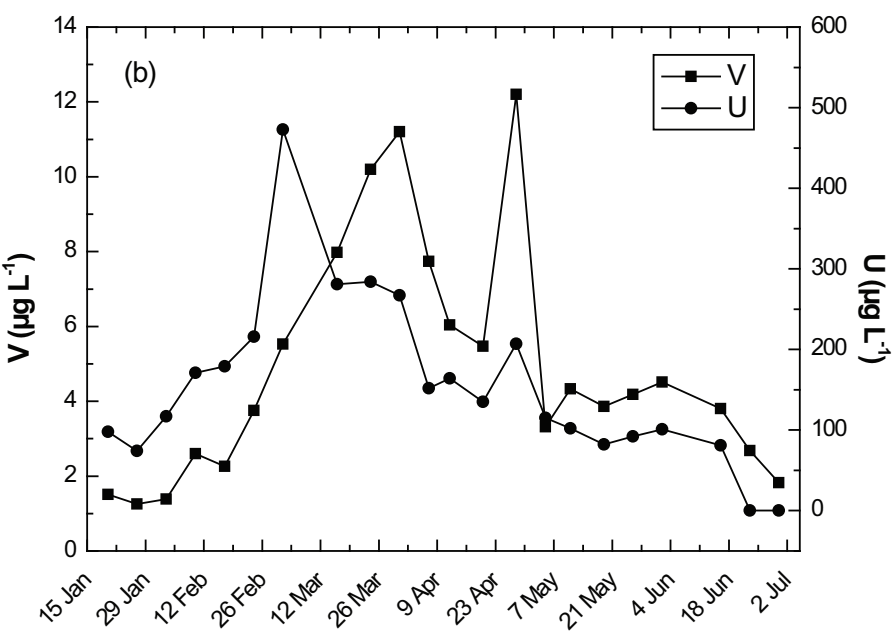
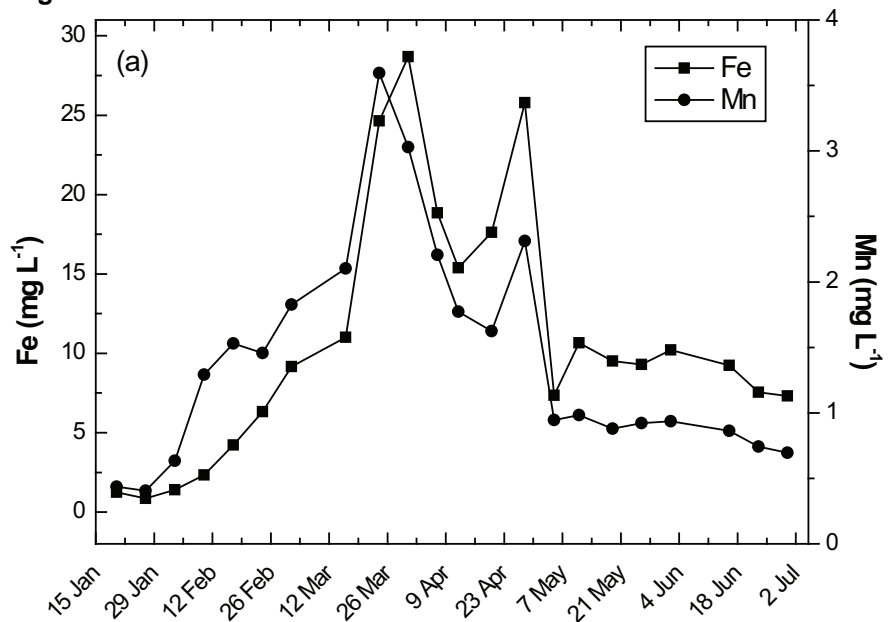
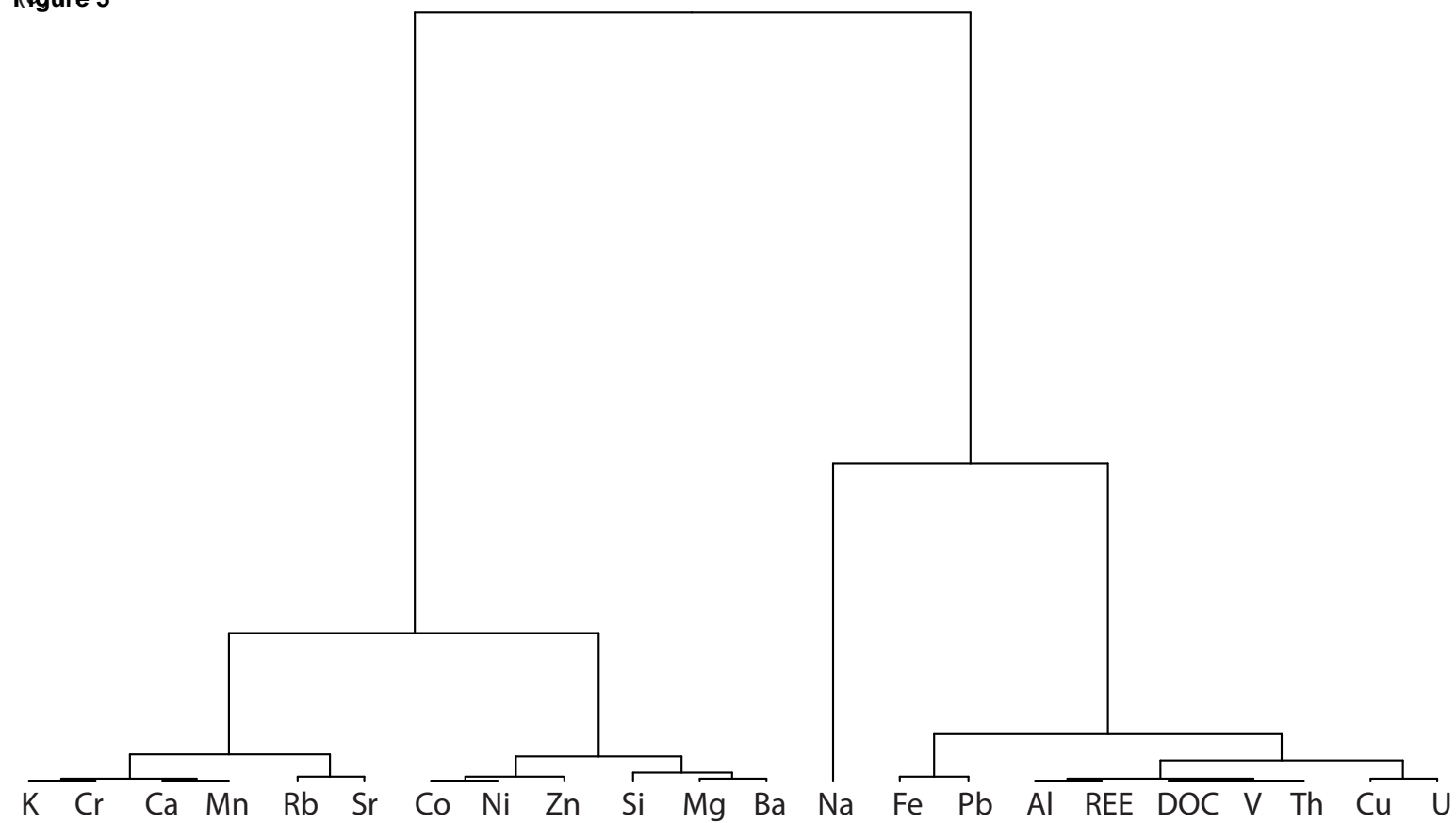


Figure 3



(b) F14

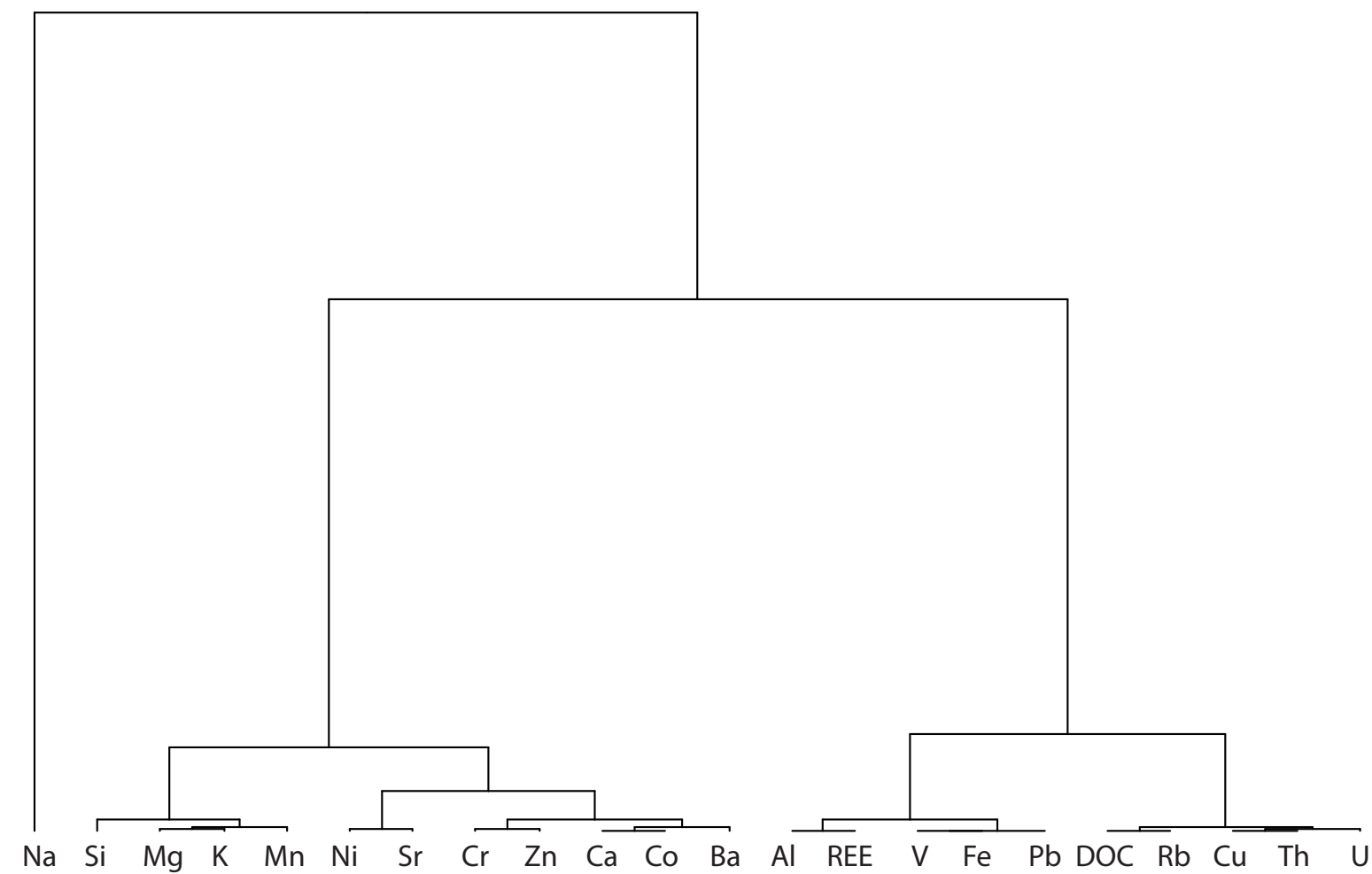


Figure 4

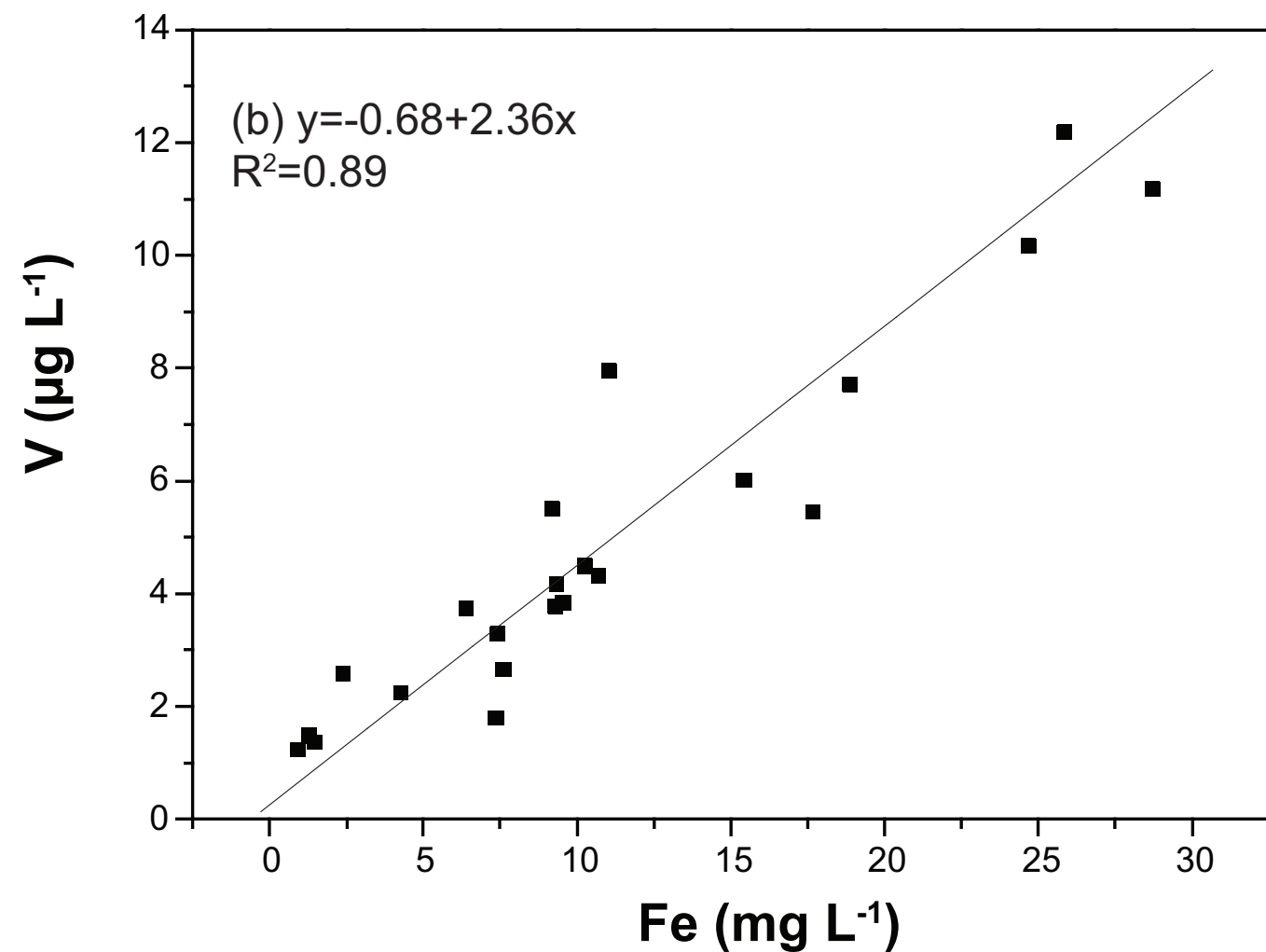
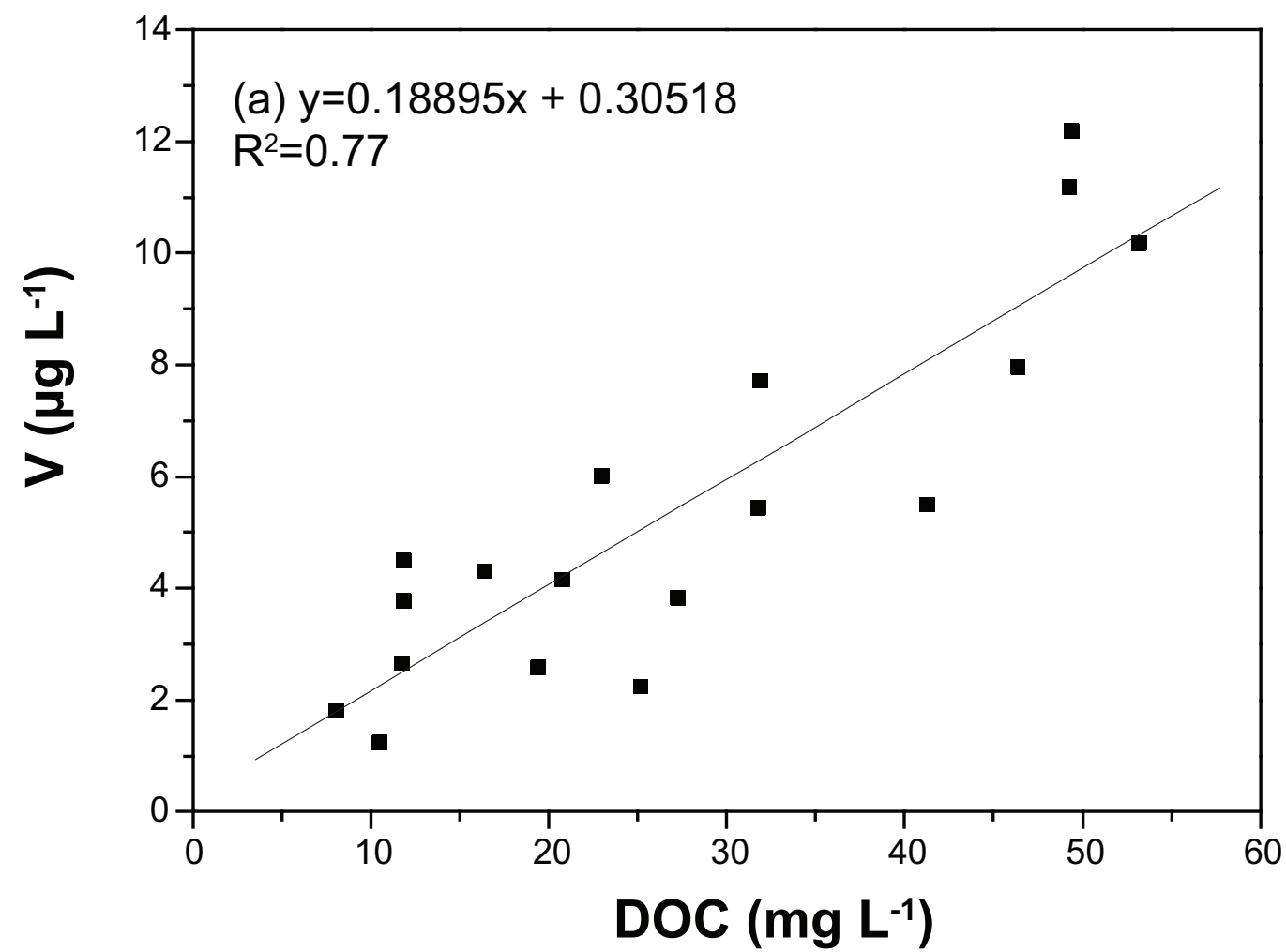


Figure 5

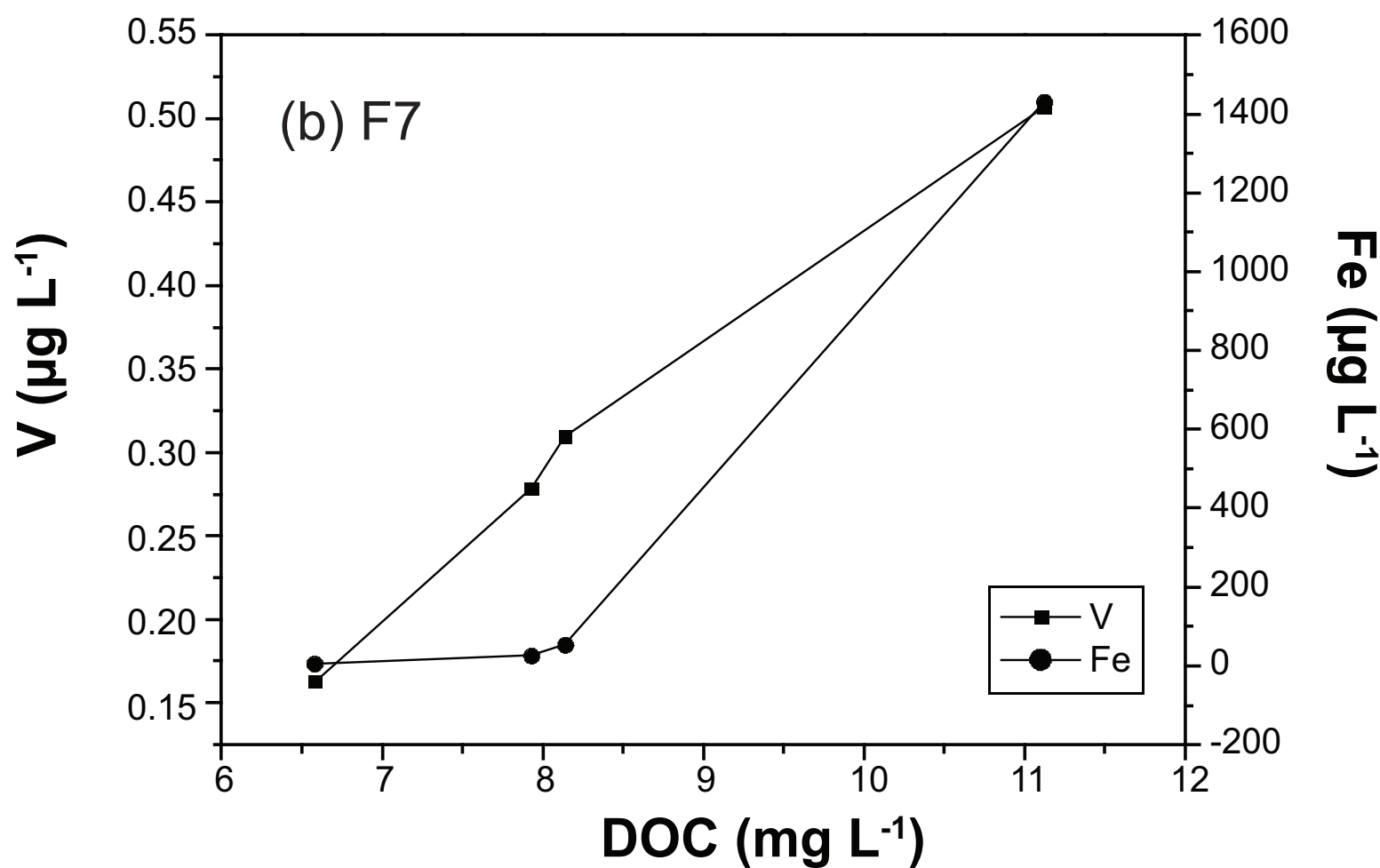
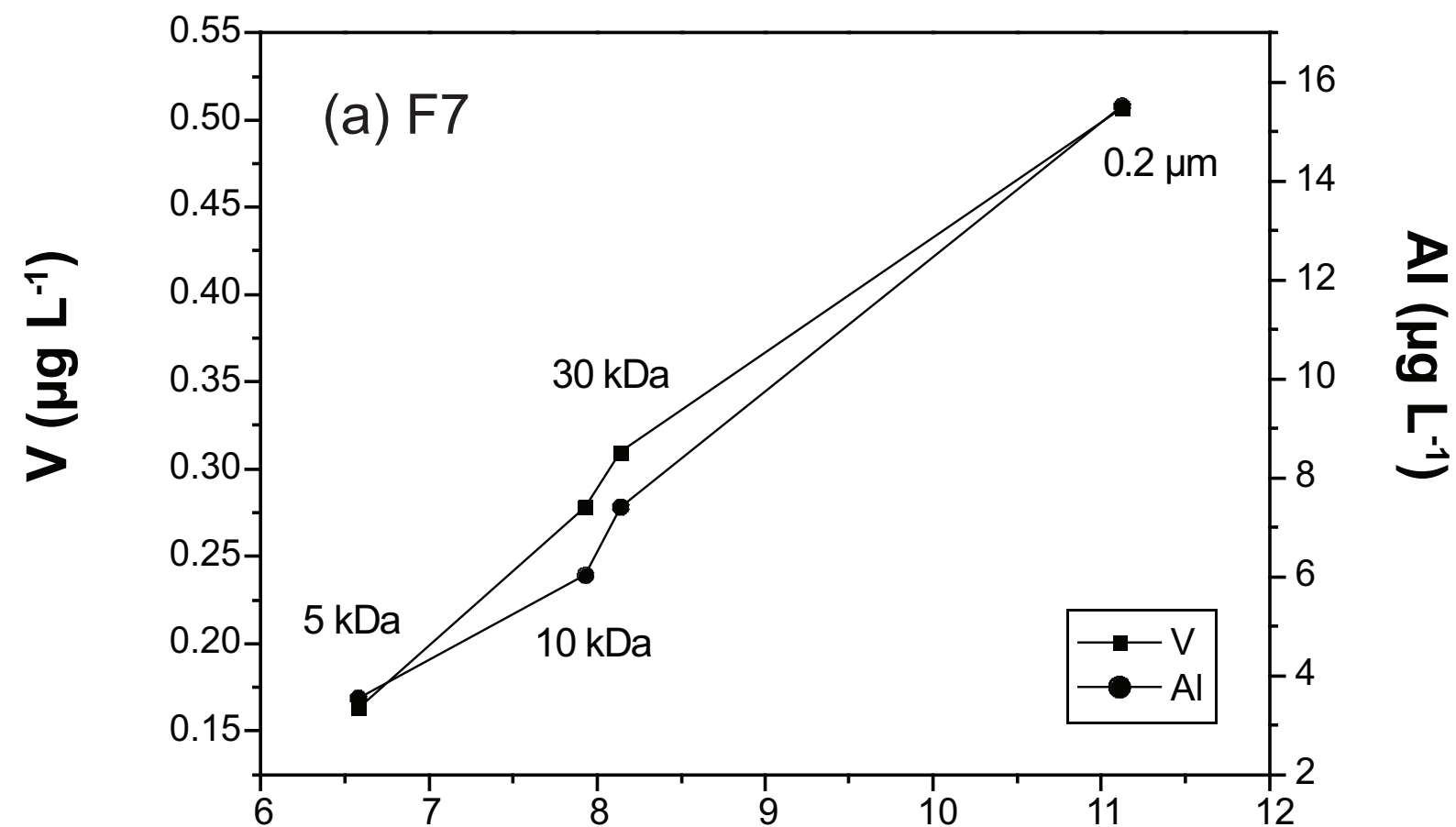
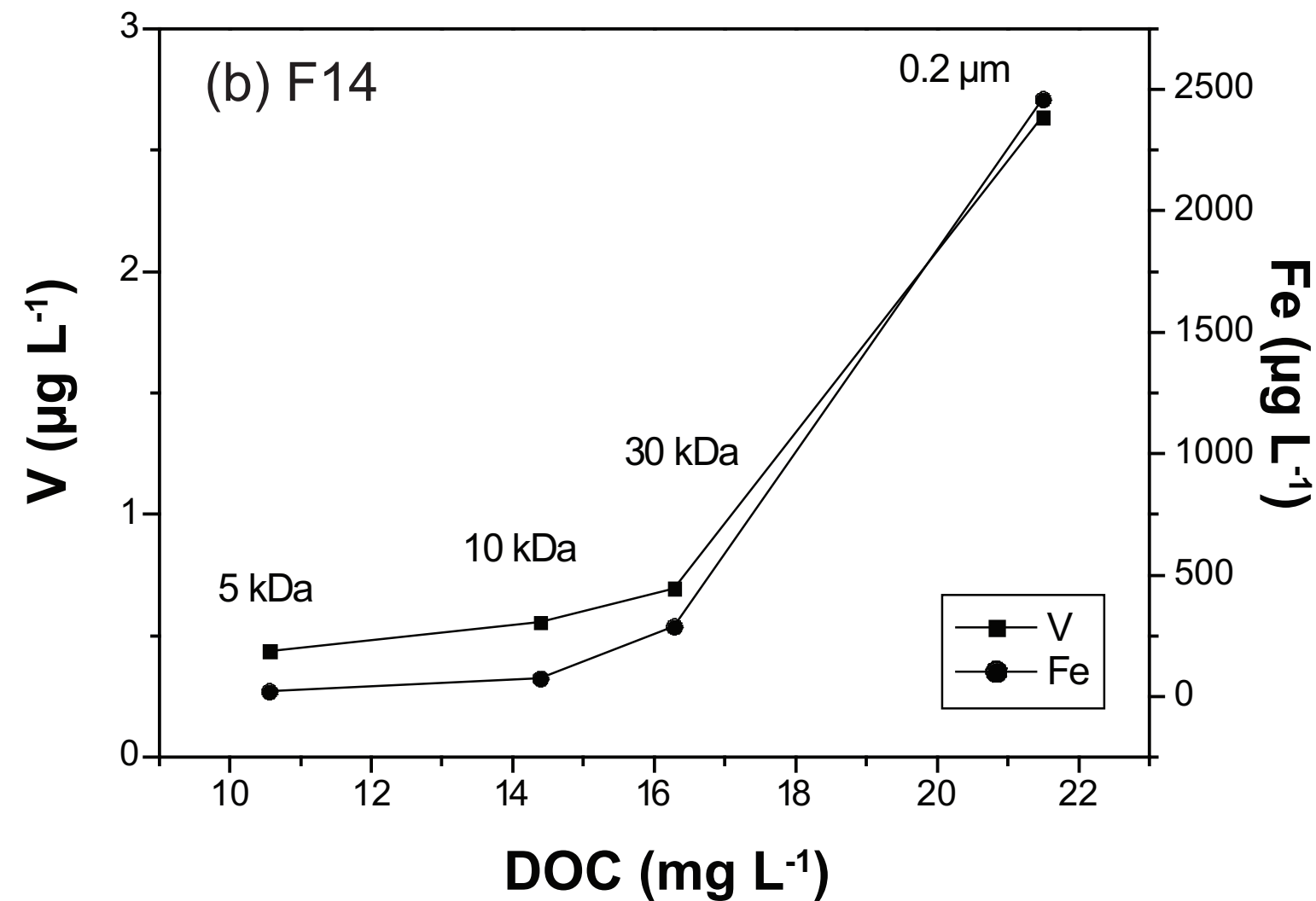
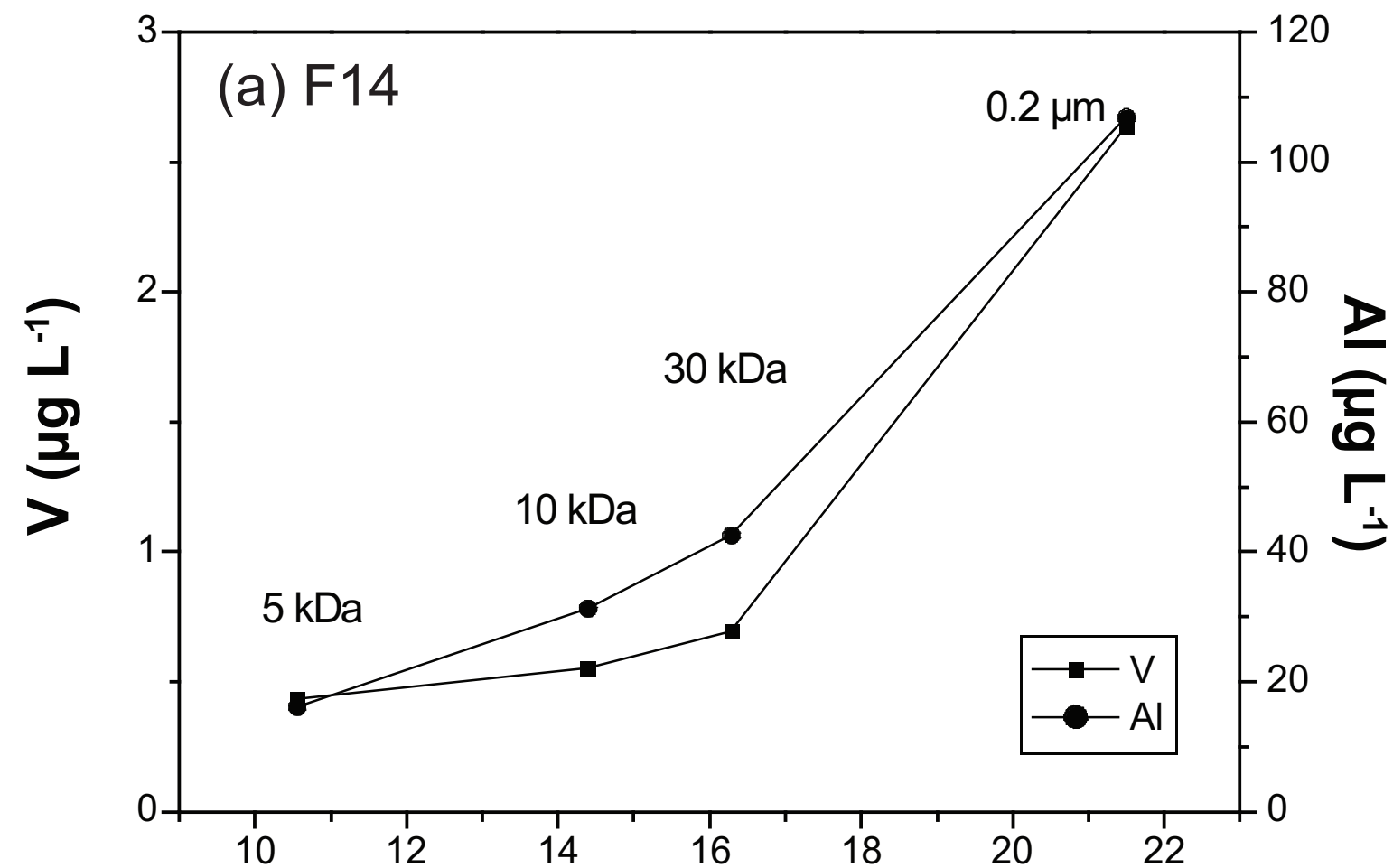
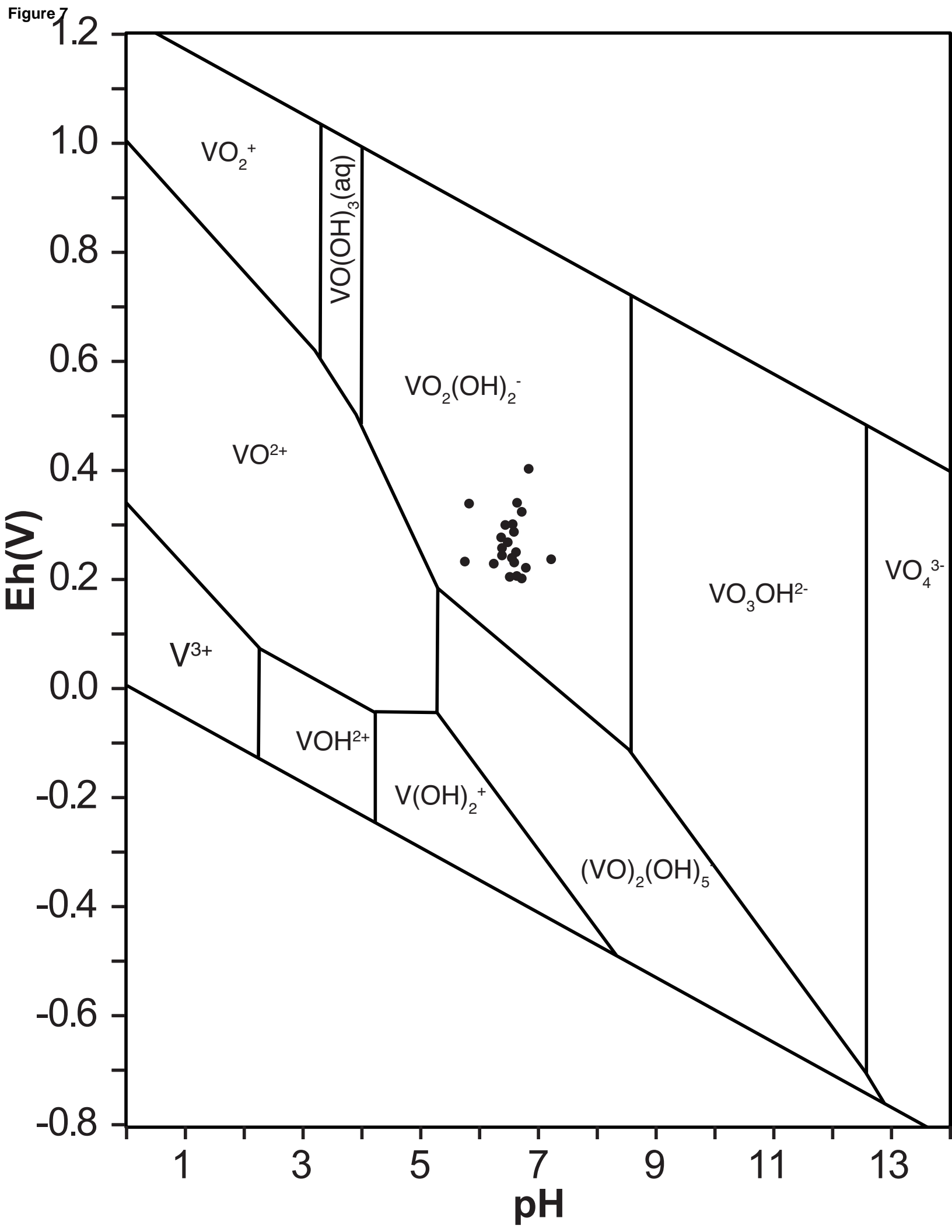


Figure 6





Parameter	Description	Values
n_A	Amount of type-A sites (mol g^{-1})	4.8×10^{-3} (FA), 3.3×10^{-3} (HA)
n_B	Amount of type-B sites (mol g^{-1})	$0.5 \times n_A$
pK_A	Intrinsic proton dissociation constant for type-A sites	3.2 (FA), 4.1 (HA)
pK_B	Intrinsic proton dissociation constant for type-B sites	9.4 (FA), 8.8 (HA)
ΔpK_A	Distribution term that modifies pK_A	3.3 (FA), 2.1 (HA)
ΔpK_B	Distribution term that modifies pK_B	4.9 (FA), 3.6 (HA)
$\log K_{MA}$	Intrinsic equilibrium constant for metal binding at type-A sites	2.4 (FA), 2.5 (HA)
$\log K_{MB}$	Intrinsic equilibrium constant for metal binding at type-B sites	$3.39 \log K_{MA} - 1.15$
ΔLK_1	Distribution term that modifies $\log K_{MA}$	2.8
ΔLK_2	Distribution term that modifies the strength of bidentate and tridentate sites	1.74 (V(IV)O)
P	Electrostatic parameter	-115 (FA), -330 (HA)
K_{sel}	Selectivity coefficient for counterion accumulation	1
f_{prB}	Fraction of proton sites that can form bidentate sites	Calculated from geometry
f_{prT}	Fraction of proton sites that can form tridentate sites	Calculated from geometry
M	Molecular weight	1.5 kDa (FA), 15 kDa (HA)
R	Molecular radius	0.8 nm (FA), 1.72 nm (HA)

Table 1.

	AlOx	FeOx	MnOx	SiOx
Γ_{\max}	8.33	8.33	8.33	8.33
pK_{H1}	6.45	6.26	0.63	(-10)
pK_{H2}	9.96	9.66	4.21	8.51
10^6 P	-1.38	-1.46	-0.88	-0.86
$\Delta \text{pK}_{\text{MH}}$	-2.2	-2	-3	-1.5
pK_{MH}	2.4	2.7	1.1	4.7

Table 2.

	P11	F5	F5	F7	F7	F14								
Date	01/20/99	02/26/98	01/20/99	02/26/98	01/20/99	01/20/99	01/27/99	02/03/99	02/10/99	02/17/99	02/24/99	03/03/99	03/16/99	03/24/99
T (°C)	11.1	n.a.	10.9	n.a.	12.7	9.4	8.1	7.6	7.0	7.6	9.1	10.1	10.1	11.5
pH	5.95	n.a.	6.05	n.a.	6.07	5.6	6.59	6.4	6.46	6.31	6.33	6.36	6.95	6.45
Eh	405	n.a.	420	n.a.	348	284	408	336	321	291	277	240	261	196
Cl	43.16	n.a.	49.46	n.a.	47.3	36.32	33.84	34.67	34.98	35.79	34.78	34.05	36.91	37.84
SO ₄	17.31	n.a.	23.61	n.a.	25.46	18.08	16.03	18.54	14.02	16.4	15.8	13.78	4.66	11
NO ₃	67.42	n.a.	69.71	n.a.	46.27	15.47	19.29	41.88	6.84	14.39	16.05	0	0	11.41
DOC	n.a.	4.4	n.a.	3.9	n.a.	n.a.	10.409	n.a.	19.313	25.136	n.a.	41.19	46.31	53.12
Na	26290	n.a.	22370	n.a.	20080	19680	18400	18430	19040	19480	18680	18820	19150	19490
Mg	10440	n.a.	14140	n.a.	12060	7033	6283	7715	7538	8376	7901	9907	10380	10710
Al	4	2	4	7	5	109	92	89	157	129	131	151	188	170
Si	8980	699	7770	808	7293	8477	7853	10340	8870	9298	9177	11560	7056	12480
K	1700	n.a.	4428	n.a.	2595	2502	2766	1522	2114	1761	1677	1225	1755	1644
Ca	15080	n.a.	21150	n.a.	18650	14310	12820	18250	17320	20050	19970	24240	21650	37610
V	0.32	0.78	0.37	1.42	0.95	1.51	1.25	1.39	2.60	2.26	3.75	5.53	7.98	10.22
Cr	2.01	4.00	1.95	2.40	0.70	1.43	1.37	1.49	1.86	1.62	1.62	2.01	2.86	2.43
Mn	29	9	12	94	65	437	405	633	1292	1530	1456	1826	2102	3595
Fe	91	93	307	168	373	1246	853	1408	2339	4220	6329	9160	11000	24640
Co	0.10	0.23	0.19	0.88	0.56	2.63	2.05	2.92	7.41	8.06	8.47	10.10	11.36	14.38
Ni	3.42	2.40	2.45	2.08	2.29	6.16	5.26	7.00	10.46	10.16	10.18	11.74	13.62	15.84
Cu	0.94	0.40	0.96	1.11	1.17	4.61	3.31	4.21	6.24	5.29	4.64	4.71	4.38	2.31
Zn	2.76	4.10	11.98	6.00	8.00	7.19	7.60	8.17	10.70	9.44	8.02	11.76	9.61	8.81
Rb	n.a.	1.13	n.a.	1.38	n.a.	n.a.	n.a.	n.a.	n.a.	n.a.	n.a.	n.a.	n.a.	n.a.
Sr	138	191	190	149	172	133	117	174	155	179	176	222	192	235
Ba	28	30	31	36	41	28	26	30	31	33	33	37	35	41
ΣREE	0.176	0.253	0.292	0.624	0.510	6.805	4.794	6.720	11.713	10.416	11.709	15.261	16.486	15.821
Pb	0.617	10.050	18.750	1.555	2.980	6.320	5.220	5.160	7.690	7.280	6.540	9.120	14.180	8.900
Th	0.110	0.011	0.135	0.038	0.230	1.850	1.400	1.680	3.180	2.760	2.740	4.280	5.340	4.950
U	0.104	0.069	0.119	0.115	0.066	0.983	0.742	1.170	1.710	1.790	2.160	4.730	2.810	2.840

Table 3. (to be continued)

n.a.: not available

	F14												
Date	03/31/99	04/07/99	04/12/99	04/20/99	04/28/99	05/05/99	05/11/99	05/19/99	05/26/99	06/02/99	06/16/99	06/23/99	06/30/99
T (°C)	12.6	11.9	10.4	11.4	13.7	14.2	13.8	13.2	16.6	13.2	17.3	18.8	16.4
pH	6.38	6.31	6.35	6.54	6.27	6.14	6.14	6	6.15	5.53	n.d.	6.23	6.21
Eh	195	223	220	220	185	231	219	196	248	170	197	245	276
Cl	39.3	35.83	34.83	34.98	29.55	33.57	34.8	34.41	32.26	32.99	32.59	31.95	31.57
SO ₄	14.05	16.76	16.71	13.56	7.56	20.2	19.21	18.74	18.23	18.04	17.29	18.93	23.5
NO ₃	9.14	8.07	0	33.56	15.6	n.a.	4.84	2.07	3.84	2.64	3.52	8.72	23.66
DOC	49.21	31.84	22.85	31.72	49.31	n.a.	16.27	27.17	20.7	11.8	11.76	11.65	7.98
Na ppb	19750	19390	19560	16860	18200	18740	18130	18130	18080	18640	17833	17330	17030
Mg	9765	8406	8300	7432	7846	7559	6922	6754	6902	7115	6875	7094	6233
Al	165	106	95	109	165	45	69	66	69	63	60	48	42
Si	12890	12940	13670	12700	9888	14870	14210	13710	13630	14150	13080	16760	15640
K	1709	1181	1123	1391	1460	575	667	658	475	489	464	497.7	516.5
Ca	34100	33630	32660	26850	32440	26560	24400	22160	23440	24220	22805	23280	21660
V	11.22	7.74	6.04	5.47	12.21	3.32	4.33	3.86	4.18	4.51	3.80	2.68	1.83
Cr	2.39	1.86	1.54	1.65	2.89	0.79	1.17	1.18	1.13	1.11	1.05	0.90	0.75
Mn	3028	2206	1773	1625	2312	945	982	880	921	935	863	742	695
Fe	28680	18840	15380	17630	25780	7355	10660	9511	9297	10220	9231	7550	7307
Co	13.74	9.71	7.68	8.45	11.58	3.92	5.29	4.95	5.36	5.27	4.95	4.32	4.47
Ni	12.05	9.73	7.87	8.09	11.73	5.46	6.55	6.40	7.00	6.72	6.41	5.83	5.46
Cu	1.90	1.40	1.32	1.15	1.95	0.63	0.87	0.98	0.89	0.80	0.83	0.76	1.12
Zn	8.13	7.26	5.98	6.32	19.33	4.60	3.99	4.07	4.23	3.59	3.84	3.53	6.99
Rb	n.a.	0.92	0.88	0.90	1.00	0.53	0.57	0.59	0.48	0.52	0.44	0.43	0.55
Sr	223	198	198	167	195	163	153	140	148	157	148	143	136
Ba	41	34	34	33	34	31	29	27	29	29	27	26	27
ΣREE	15.655	10.514	9.255	n.a.	15.479	6.921	8.373	6.791	7.854	8.132	6.744	5.633	4.406
Pb	8.750	5.310	4.590	7.340	11.480	2.260	3.710	3.600	3.480	2.880	2.682	0.002	0.002
Th	5.000	2.200	1.890	2.390	3.930	1.010	1.520	1.230	1.330	1.320	1.190	1.100	0.771
U	2.670	1.520	1.640	1.350	2.070	1.150	1.020	0.823	0.922	1.010	0.811	0.001	0.001

Table 3.

n.a.: not available

	F7							F14						
	0.2 μ m	30 kDa	30 kDa	10 kDa	10 kDa	5 kDa	5 kDa	0.2 μ m	30 kDa	30 kDa	10 kDa	10 kDa	5 kDa	5 kDa
T (°C)	10.6							10.4						
pH	6.19							6.40						
Cl	69							53						
SO ₄	62							35						
NO ₃	1							1						
Alkalinity	1.318							623						
DOC	11.1	8.2	8.1	8.0	7.8	6.9	6.3	21.5	16.3	16.2	14.7	14.1	10.6	10.5
Na	35,090	40,830	40,830	35,410	35,410	37,650	37,650	24,000	22,260	24,810	24,760	24,030	19,882	19,494
Mg	12,150	12,780	13,000	15,680	11,450	12,160	11,510	7,613	6,738	7,460	7,332	7,297	6,222	6,064
Al	16	10	9	9	7	8	5	107	41	44	33	30	16	16
Si	14,220	15,050	15,730	18,420	13,860	14,740	13,740	12,860	11,610	13,190	13,110	12,705	11,674	11,294
K	463	477	531	603	463	445	405	895	845	895	902	873	809	772
Ca	30,800	32,270	34,840	40,370	30,850	31,600	29,570	24,880	23,220	24,730	24,290	23,648	22,389	21,481
V	0.51	0.29	0.32	0.37	0.28	0.35	0.25	2.64	0.68	0.72	0.57	0.55	0.46	0.42
Cr	0.91	1.07	1.20	1.35	1.03	0.95	0.82	1.71	1.44	1.51	1.32	1.22	0.83	0.73
Mn	1,193	1,239	1,316	1,572	1,178	1,206	1,135	512	417	436	430	418	13	13
Fe	1.431	373	372	46	51	30	22	2,462	275	305	83	69	20	26
Co	6.72	6.84	7.34	8.20	6.22	6.15	5.51	4.74	3.46	3.72	3.46	3.31	0.14	0.14
Ni	11.72	11.79	12.67	13.81	10.46	9.62	7.98	11.71	9.54	14.54	10.97	8.93	6.53	6.60
Cu	2.52	2.29	2.43	2.39	1.83	1.87	1.38	10.19	7.42	7.90	6.51	5.69	4.73	4.50
Zn	8.43	7.45	8.62	9.55	7.41	7.60	6.60	12.41	10.99	9.27	9.26	8.41	5.72	5.31
Rb	1.72	1.76	1.92	2.28	1.75	1.72	1.60	0.88	0.86	0.88	0.88	0.85	0.87	0.85
Sr	189.60	195.80	212.30	259.30	193.70	196.90	184.90	155.10	149.50	159.90	152.60	148.21	144.53	143.03
Ba	51.20	51.38	56.42	66.37	51.62	49.76	46.72	34.21	29.95	29.75	29.42	28.83	22.39	21.81
ΣREE	3.793	1.539	1.796	1.625	1.220	1.407	0.663	8.649	2.777	2.778	1.746	1.557	0.651	0.656
Pb	0.057	0.031	0.006	0.002	0.031	0.027	0.026	1.195	0.096	0.085	0.011	0.013	0.023	0.018
Th	0.037	0.019	0.019	0.015	0.011	0.007	0.003	0.163	0.098	0.099	0.060	0.049	0.013	0.013
U	0.061	0.049	0.051	0.051	0.039	0.038	0.029	0.118	0.067	0.065	0.045	0.039	0.017	0.017

Table 4.

	<i>HA</i>	<i>FA</i>	<i>Inorganic</i>
F7	47	47	6
F14	58	41	1

Table 5.